

Soil Moisture Active Passive (SMAP) Project: Calibration and Validation for the L2/3_SM_P Version 6 and L2/3_SM_P_E Version 3 Data Products

Citation:

O'Neill, P.², S. Chan³, R. Bindlish², M. Chaubell³, A. Colliander³, F. Chen¹, S. Dunbar³, T. Jackson¹, J. Piepmeier², S. Misra³, M. Cosh¹, T. Caldwell⁴, J. Walker⁵, X. Wu⁵, A. Berg⁶, T. Rowlandson⁶, A. Pacheco⁷, H. McNairn⁷, M. Thibeault⁸, J. Martínez-Fernández⁹, Á. González-Zamora⁹, E. Lopez-Baeza¹⁰, F. Udall¹¹, M. Seyfried¹², D. Bosch¹³, P. Starks¹⁴, C. Holifield¹⁵, J. Prueger¹⁶, Z. Su¹⁷, R. van der Velde¹⁷, J. Asanuma¹⁸, M. Palecki¹⁹, E. Small²⁰, M. Zreda²¹, J. Calvet²², W. Crow¹, Y. Kerr²³, S. Yueh³, and D. Entekhabi²⁴, August 15, 2019. *Calibration and Validation for the L2/3_SM_P Version 6 and L2/3_SM_P_E Version 3 Data Products*, SMAP Project, JPL D-56297, Jet Propulsion Laboratory, Pasadena, CA.

Paper copies of this document may not be current and should not be relied on for official purposes. The current version is in the Product Data Management System (PDMS): <https://pdms.jpl.nasa.gov/>

August 15, 2019

JPL D-56297

National Aeronautics and Space Administration



Jet Propulsion Laboratory
4800 Oak Grove Drive
Pasadena, California 91109-8099
California Institute of Technology

Copyright 2019 California Institute of Technology. U.S. Government sponsorship acknowledged.

Contributors to this report:

O'Neill, P.², S. Chan³, R. Bindlish², M. Chaubell³, A. Colliander³, F. Chen¹, S. Dunbar³, T. Jackson¹, J. Piepmeier², S. Misra³, M. Cosh¹, T. Caldwell⁴, J. Walker⁵, X. Wu⁵, A. Berg⁶, T. Rowlandson⁶, A. Pacheco⁷, H. McNairn⁷, M. Thibeault⁸, J. Martínez-Fernández⁹, Á. González-Zamora⁹, E. Lopez-Baeza¹⁰, F. Udall¹¹, M. Seyfried¹², D. Bosch¹³, P. Starks¹⁴, C. Holifield¹⁵, J. Prueger¹⁶, Z. Su¹⁷, R. van der Velde¹⁷, J. Asanuma¹⁸, M. Palecki¹⁹, E. Small²⁰, M. Zreda²¹, J. Calvet²², W. Crow¹, Y. Kerr²³, S. Yueh³, and D. Entekhabi²⁴.

¹USDA ARS Hydrology and Remote Sensing Lab, Beltsville, MD 20705 USA

²NASA Goddard Space Flight Center, Greenbelt, MD 20771 USA

³Jet Propulsion Laboratory, California Institute of Technology, Pasadena, CA 91109 USA

⁴U.S. Geological Survey, Nevada Water Science Center 89701 USA

⁵Monash University, Clayton, Australia

⁶University of Guelph, Guelph, Canada

⁷Agriculture and Agri-Food Canada, Ottawa, Canada

⁸Comisión Nacional de Actividades Espaciales (CONAE), Buenos Aires, Argentina

⁹University of Salamanca, Salamanca, Spain

¹⁰University of Valencia, Valencia, Spain

¹¹Center for Hydrology, Technical University of Denmark, Copenhagen, Denmark

¹²USDA ARS Northwest Watershed Research Center, Boise, ID 83712 USA

¹³USDA ARS Southeast Watershed Research Center, Tifton, GA 31793 USA

¹⁴USDA ARS Grazinglands Research Laboratory, El Reno, OK 73036 USA

¹⁵USDA ARS Southwest Watershed Research Center, Tucson, AZ 85719 USA

¹⁶USDA ARS National Laboratory for Agriculture and the Environment, Ames, IA 50011 USA

¹⁷University of Twente, Enschede, Netherlands

¹⁸University of Tsukuba, Tsukuba, Japan

¹⁹NOAA National Climatic Data Center, Asheville, NC 28801 USA

²⁰University of Colorado, Boulder, CO 80309 USA

²¹University of Arizona, Tucson, AZ 85751 USA

²²CNRM-GAME, UMR 3589 (Météo-France, CNRS), Toulouse, France

²³CESBIO-CNES, Toulouse, France

²⁴Massachusetts Institute of Technology, Cambridge, MA 02139 USA

This research was carried out at the Jet Propulsion Laboratory, California Institute of Technology, under a contract with the National Aeronautics and Space Administration. © 2019. All rights reserved.

TABLE OF CONTENTS

| | | |
|------------|---|-----------|
| 1 | EXECUTIVE SUMMARY | 4 |
| 2 | OBJECTIVES OF CAL/VAL | 6 |
| 3 | Brief Description of the L2SMP and L2SMP_E..... | 8 |
| 4 | L1 RADIOMETER PRODUCT UPDATES | 9 |
| 4.1 | Water Body Correction | 11 |
| 5 | ALTERNATIVE L2SMP/L2SMP_E ALGORITHMS..... | 12 |
| 5.1 | Single Channel Algorithm V-pol (SCA-V) | 12 |
| 5.2 | Single Channel Algorithm H-pol (SCA-H) | 12 |
| 5.3 | Modified Dual Channel Algorithm (MDCA) | 13 |
| 5.4 | Effective Temperature Methodology | 13 |
| 6 | METHODOLOGIES USED FOR L2SMP/L2SMP_E CAL/VAL | 14 |
| 6.1 | Validation Grid (VG)..... | 14 |
| 7 | SUMMARY OF REFINEMENTS IN L2SMP VERSION 6 and L2SMP_E VERSION 3 AND VALIDATION | 16 |
| 8 | ASSESSMENTS | 17 |
| 8.1 | L2SMP | 17 |
| 8.1.1 | Core Validation Sites | 17 |
| 8.1.2 | Sparse Networks | 24 |
| 8.2 | L2SMP_E..... | 28 |
| 8.2.1 | Core Validation Sites | 28 |
| 8.2.2 | Sparse Networks | 28 |
| 8.3 | Summary..... | 33 |
| 9 | OUTLOOK AND FUTURE PLANS | 34 |
| 10 | ACKNOWLEDGEMENTS | 36 |
| 11 | REFERENCES | 37 |
| 12 | BIBLIOGRAPHY OF PUBLISHED SMAP L2SMP and L2SMP_E VALIDATION STUDIES..... | 39 |

1 EXECUTIVE SUMMARY

During the post-launch Cal/Val Phase of SMAP there are two objectives for each science product team: 1) calibrate, verify, and improve the performance of the science algorithms, and 2) validate accuracies of the current release of the science data products as specified in the L1 science requirements according to the Cal/Val timeline. This report provides analysis and assessment of the SMAP Level 2 Soil Moisture Passive (L2SMP) Version 6 and the L2SMP Enhanced (L2SMP_E) Version 3 data products. The L2SMP product is provided on a 36-km grid and the L2SMP_E on a 9-km grid. The SMAP Level 3 Soil Moisture Passive (L3SMP, L3SMP_E) products are simply a daily composite of the L2 half-orbit files. Hence, analysis and assessment of the L2SMP and L2SMP_E products can also be considered to cover the L3SMP and L3SMP_E products.

The new versions of the passive soil moisture products replace the dual channel retrieval algorithm (DCA) with an alternative modified dual channel algorithm (MDCA) which shows a significant improvement over the original DCA. **The baseline algorithm (SCA-V) remains unchanged for both Level-2 and Level-3 products and continues to have the best performance metrics.**

Assessment methodologies utilized include comparisons of SMAP soil moisture retrievals with *in situ* soil moisture observations from core validation sites (CVS) and sparse networks, and intercomparison with products from ESA's Soil Moisture Ocean Salinity (SMOS) mission. The primary assessment methodology is the CVS comparisons using established metrics and time series plots. These metrics include unbiased root mean square error (ubRMSE), bias, mean absolute bias (MAB), and correlation. The ubRMSE captures time-random errors, bias and MAB capture the mean differences or offsets, and correlation captures phase compatibility between data series. It should be noted that some changes have been made in the calibration and upscaling of select CVS based upon follow-up investigations by Cal/Val Partners. In addition, the assessment period is now 48 months (as opposed to 36 months in the L2SMP Version 5 and L2SMP_E Version 2 assessments [1]).

SMAP L2SMP supports a total of three alternative retrieval algorithms: the Single Channel Algorithm–H polarization (SCA-H), Single Channel Algorithm–V polarization (SCA-V), and Modified Dual Channel Algorithm (MDCA) are the focus of this assessment. These same retrieval algorithms were also used in evaluating the performance of L2SMP_E.

The first step in assessment was the comparison of the L2SMP AM (Descending) and PM (Ascending) Version 6 products to the CVS and sparse network observations. CVS (AM) results indicated that the SCA-V provided the best overall performance with an ubRMSE of $0.038 \text{ m}^3/\text{m}^3$, bias of $0.001 \text{ m}^3/\text{m}^3$ and correlation of 0.822. These metrics exceed the SMAP mission requirements and those of the SMOS products. A portion of the change in the metrics may be associated with the longer period of record (36 vs 48 months) since longer records may include a wider range of anomalous conditions or a more typical set of conditions. Sparse network results confirmed the trends seen in the CVS comparisons. The overall conclusion is that the L2SMP AM and PM products have improved performance with a reduction in bias and ubRMSE that exceeds the mission accuracy requirements for L2 passive retrieved soil moisture (the L2SMP soil moisture shall meet or exceed an accuracy of $0.040 \text{ m}^3/\text{m}^3$ ubRMSE over land in the absence of frozen ground, permanent snow/ice, or dense vegetation; this requirement is actually written for retrieved soil moisture at 10 km spatial resolution, but has been applied by the SMAP team to all L2 passive soil moisture products). The combination of analyses using the CVS and sparse networks, intercomparison with products from the SMOS mission, and recent triple collocation analyses have contributed to a better understanding of the performance uncertainties. The assessment now includes 48 months of intercomparisons, and several papers have been published in peer-reviewed journals [2-5] as well as numerous investigations listed in the Bibliography section of the report. These analyses satisfy the criteria established by the Committee on Earth Observing Satellites (CEOS) for Stage 4 validation.

The L2SMP_E are posted at 9 km but the contributing domain (i.e. primary spatial area contributing to the radiometer brightness temperature response) is larger than this, approximately 33 km. A different set of CVS domains than those used for the L2SMP were identified in order to assess the performance of the L2SMP_E product; all ground measurements of soil moisture within the 33-km domain were used and compared to the SMAP retrieved soil moisture at each CVS. Additional information on the L2SMP_E product can be found in [1].

Version 3 of the L2SMP_E, for both AM and PM orbits, was assessed using the CVS and sparse networks. Both the AM and PM products meet the mission requirements and reflect the patterns for L2SMP. SCA-V had the best overall metrics of all the retrieval algorithms with an ubRMSE of 0.038 m³/m³, bias of -0.002 m³/m³ and correlation of 0.817 for AM orbits, and an ubRMSE of 0.036 m³/m³, bias of -0.002 m³/m³ and correlation of 0.825 for the PM orbits. MDCA not only shows a significant improvement with respect to the previous DCA version but its performance now also satisfies the mission accuracy requirements. MDCA performance shows an ubRMSE of 0.040 m³/m³, bias of -0.007 m³/m³ and correlation of 0.772 for AM orbits, and an ubRMSE of 0.039 m³/m³, bias of -0.013 m³/m³ and correlation of 0.760 for the PM orbits. For the same reasons noted for the L2SMP, the maturity of the L2SMP_E product is now at CEOS Stage 4.

Overall conclusions in this assessment:

- L2SMP and L2SMP_E performances continue to meet project target accuracy (0.040 m³/m³ ubRMSE or better).
- MDCA outperforms the original DCA and meets project target accuracy (0.040 m³/m³ ubRMSE or better).
- SCA-V continues to outperform the alternative algorithms.
- Both the L2SMP and L2SMP_E products have achieved CEOS Validation Stage 4.

2 OBJECTIVES OF CAL/VAL

During the post-launch Cal/Val (Calibration/Validation) Phase of SMAP there are two objectives for each science product team:

- Calibrate, verify, and improve the performance of the science algorithms, and
- Validate accuracies of the science data products as specified in Level 1 science requirements according to the Cal/Val timeline.

The process is illustrated in Figure 2.1. In this Assessment Report the progress of the Level 2 Soil Moisture Passive Team in addressing these objectives is described. The approaches and procedures utilized follow those described in the SMAP Cal/Val Plan [6] and Algorithm Theoretical Basis Document for the Level 2 & 3 Soil Moisture (Passive) Data Products [7].

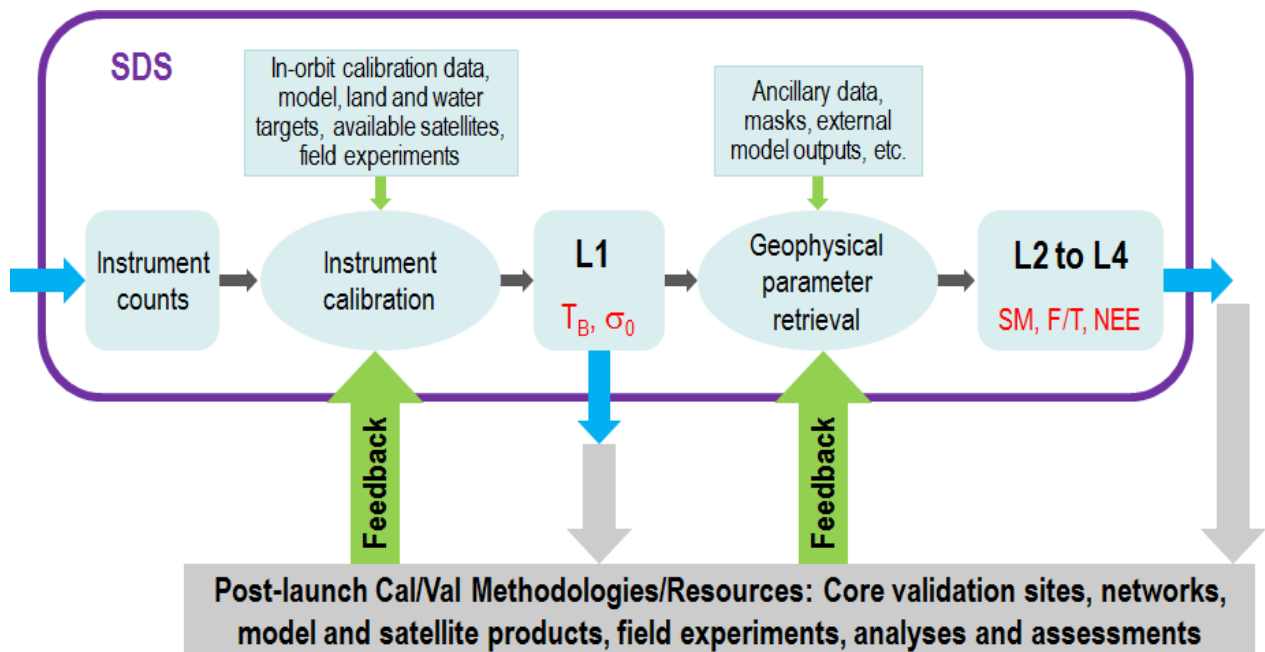


Figure 2.1. Overview of the SMAP Cal/Val Process.

SMAP established a unified definition base in order to effectively address the mission requirements. These are documented in the SMAP Handbook/ Science Terms and Definitions [8], where Calibration and Validation are defined as follows:

- *Calibration*: The set of operations that establish, under specified conditions, the relationship between sets of values or quantities indicated by a measuring instrument or measuring system and the corresponding values realized by standards.
- *Validation*: The process of assessing by independent means the quality of the data products derived from the system outputs.

The L2SMP Team adopted the same soil moisture retrieval accuracy requirement for the fully validated L2SMP data ($0.040 \text{ m}^3/\text{m}^3$) that is listed in the L1 Mission Requirements Document [9] for the active/passive soil moisture product.

In assessing the maturity of the L2SMP (and L2SMP_E) products, the team considered the guidance provided by the Committee on Earth Observation Satellites (CEOS) Working Group on Calibration and Validation (WGCV) [10]:

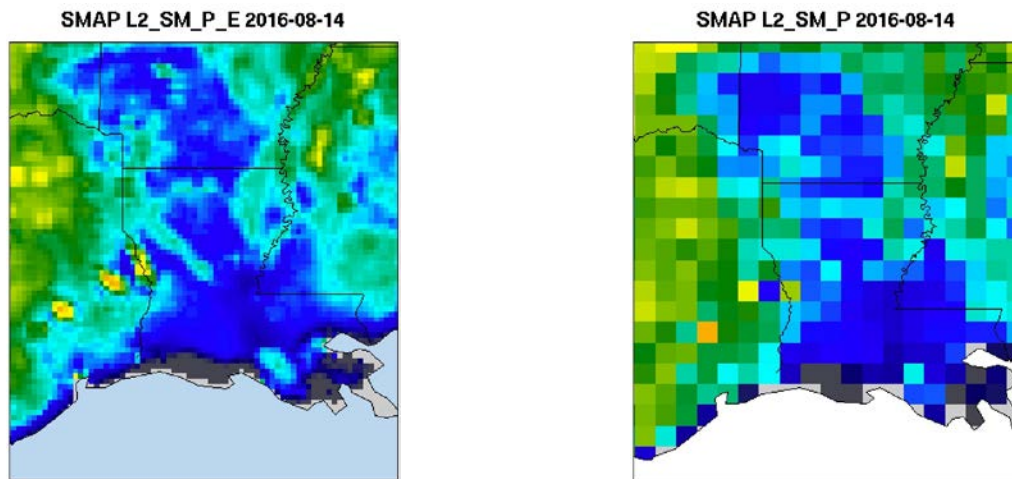
- Stage 1: Product accuracy is assessed from a small (typically < 30) set of locations and time periods by comparison with *in situ* or other suitable reference data.
- Stage 2: Product accuracy is estimated over a significant set of locations and time periods by comparison with reference *in situ* or other suitable reference data. Spatial and temporal consistency of the product and with similar products has been evaluated over globally representative locations and time periods. Results are published in the peer-reviewed literature.
- Stage 3: Uncertainties in the product and its associated structure are well quantified from comparison with reference *in situ* or other suitable reference data. Uncertainties are characterized in a statistically robust way over multiple locations and time periods representing global conditions. Spatial and temporal consistency of the product and with similar products has been evaluated over globally representative locations and periods. Results are published in the peer-reviewed literature.
- Stage 4: Validation results for stage 3 are systematically updated when new product versions are released and as the time series expands.

Based on the extensive validation analyses to date, the number of peer reviewed publications as well as numerous investigations listed in the Bibliography section of the report, the length of the SMAP period of record, and the utilization of feedback of validation in a systematic update, with this Version of L2SMP and L2SMP_E the team has completed Stage 4. The Cal/Val program will continue with the goals of increasing the robustness of the soil moisture products and addressing specific site issues.

3 BRIEF DESCRIPTION OF THE L2SMP AND L2SMP_E

The L2SMP product is derived using SMAP L-band radiometer time-ordered observations (L1CTB product) as the primary input [7] along with other ancillary data on finer grid resolutions, to retrieve soil moisture (and other geophysical parameters as applicable) from a forward model. The resulting soil moisture retrieval output fields, along with others carrying supplementary geolocation information, brightness temperatures, quality flags, and ancillary data, are posted on a 36-km Earth-fixed grid using the global cylindrical Equal-Area Scalable Earth Grid projection, Version 2 (EASEv2). The 36-km grid resolution is close to the 3-dB native spatial resolution of the instrument observations. The use of the fixed grid facilitates temporal analyses and ingestion of the products into some user applications. However, it presents challenges to validation given that many core validation sites (CVS) are not centered or contained in a single 36-km EASE grid cell. As a result, a shifted variation of the L2SMP grid is used for validation and assessment purposes (Validation Grid-VG).

Following the SMAP launch, methodologies for improving the spatial information of the SMAP radiometer products were explored that resulted in the L1CTB_E (Enhanced) product. Backus-Gilbert (BG) optimal interpolation methodology is used that takes advantage of the radiometer oversampling on orbit. The processing results in data at a higher spatial density by virtue of TB interpolation at a 9-km grid resolution in L1BTB_E. It is important to note that the L1CTB_E processing does not improve the native resolution (~36 km) of the original TB measurements acquired by the SMAP radiometer. It is a posting of data interpolated to a 9-km grid, which can enhance spatial information (see Figure 3.1). The fine grid resolution (9 km) of L1CTB_E provides a convenient basis to produce passive soil moisture retrieval at the same fine grid resolution. Operationally, this is achieved by applying the same soil moisture inversion algorithms used for the standard 36-km L2SMP product to the enhanced 9-km L2SMP_E product. The 9-km posting provides more flexibility in co-locating the grids and CVS data and therefore does not require the use of the VG in validation and assessment of the L2SMP_E product.



(a) Enhanced Passive Soil Moisture Product

(b) Standard Passive Soil Moisture Product

Figure 3.1. Compared with the current standard L2SMP soil moisture product in (b), the enhanced L2SMP_E soil moisture product in (a) demonstrates a more detailed distribution of surface soil moisture and shows spatial features more clearly than does the standard product.

4 L1 RADIOMETER PRODUCT UPDATES

The L2SMP soil moisture retrievals are based on the 2018 Version 4 of the radiometer Level 1B and 1C brightness temperature data [<http://nsidc.org/data/smap/smap-data.html>]. An assessment of data quality and calibration is available at NSIDC [http://nsidc.org/data/docs/daac/smap/sp_11b_tb/index.html] representing the 2018 release, from which the material in this section is drawn. A more detailed discussion of the radiometer calibration and products can be found in [11,12,13]. The Version 4 TB data meet the noise equivalent delta temperature (NEDT) and geolocation requirements with margin as they did in Version 3 (see Table 4.1) [14].

The SMAP L1 radiometer calibration algorithm for the Version 4 release in 2018 was significantly revised compared to the Version 3 dataset. The calibration changes can be summarized as follows: (1) revised SMAP reflector emissivity values, (2) concurrent antenna pattern correction (APC), noise-diode, and reference load calibration, and (3) improved galaxy correction model over the ocean. It is anticipated that another revision of the SMAP L1 radiometer calibration algorithm will occur in 2020; in the meantime, the 2018 release radiometer calibration is being used for all L2 passive soil moisture products.

The SMAP radiometer calibration procedure adjusted V and H-pol microwave emissivity values for the reflector based on antenna temperature deviations observed during annual SMAP eclipse seasons. An emissivity correction slightly impacts the gain and bias of the radiometer front-end antenna temperatures. In addition to an emissivity correction, SMAP implemented an optimized concurrent calibration scheme that utilizes cold-sky looks with ocean back-lobes, cold-sky looks with ocean/land transition back-lobes, vicarious global mean ocean observations, and nadir ocean and land observations. The retrieved noise-diode temperature, reference load temperature and APC value calibration coefficients along with ocean bias correction provide a completely bias free full-range SMAP calibration. The final calibration correction for ocean regions is a reflected galaxy correction upgrade, where wind speed-dependent sky maps are used to correct for any galaxy contribution into the antenna temperature. Any previously observed fore-aft differences in L1C_TB radio frequency interference (RFI) still remain. The RFI behavior is similar as before: conditions in the Americas and Europe are good with poorer conditions in Asia.

These changes in SMAP calibration resulted in a change in metrics when comparing SMAP TB to SMOS TB. Global average brightness temperature comparisons over land areas are now 1.15 K (for H pol) and 0.66 K (for V pol) greater than SMOS (mean difference at top of the atmosphere after Faraday rotation correction was applied). In summary, the radiometer calibration is very stable over time, and changes in agreement with SMOS are consistent with intentional calibration changes in SMAP data. The noise and geolocation performance meet requirements with margin. Excellent performance should be expected over homogeneous land surfaces.

Table 4.1. Version 3* Characteristics of SMAP L1 Radiometer Data
(*now superseded by Version 4)

| Parameter | | Mission Requirement |
|-----------------------------|---------|----------------------|
| NEDT ¹ | 1.1 K | < 1.6 K ¹ |
| Geolocation accuracy | 2.7 km | < 4 km |
| Land SMAP/SMOS bias (H pol) | -2.65 K | n/a |
| Land SMAP/SMOS bias (V pol) | -2.71 K | n/a |

¹An NEDT of 1.6 K for a single-look L1B_TB footprint is equivalent to an NEDT of 0.51 K on a 30 x 30 km grid (Table 2.1 in SMAP Radiometer Error Budget, JPL D-61632 [14]). When combined with other error terms in

It is a challenge to validate brightness temperatures over land targets due to the heterogeneity of the land surface. SMOS L1 brightness temperature provides an opportunity to check the consistency in brightness temperature between the two L-band missions. SMOS has in general benefitted from more extensive Cal/Val activities than SMAP due to its relative longevity in operational data acquisition (SMOS launched in November 2009). SMOS observations at the top of the atmosphere were reprocessed to 40° incidence angle (after applying Faraday rotation correction). SMAP L1B observations were co-located with reprocessed SMOS observations (only SMAP and SMOS observations acquired less than 30 minutes apart were used). The current L1B radiometer data (T15560) were compared with the most recent SMOS L1B data (version 620) for this analysis.

Figure 4.1 shows the density plot of the brightness temperature (top of the atmosphere) comparison between SMOS and SMAP over land targets for V-pol and H-polarization. SMOS and SMAP observations show a very strong correlation over land targets (Table 4.2). SMAP observations show a warmer TB bias (about 0.66 K for V pol and 1.15 K for H pol) as compared to SMOS for both polarizations. Most of the RMSD can be attributed to the bias between the two satellites. Global average brightness temperature comparisons over ocean areas with SMOS are quite favorable indicating less than 0.25 K mean bias at top of the atmosphere. Efforts will be made to address these differences in TB calibration and to develop a consistent L-band brightness temperature dataset between SMOS and SMAP missions. The impact of these TB differences on soil moisture comparisons between the two satellites is more complex because the two missions use different soil moisture algorithms and ancillary datasets.

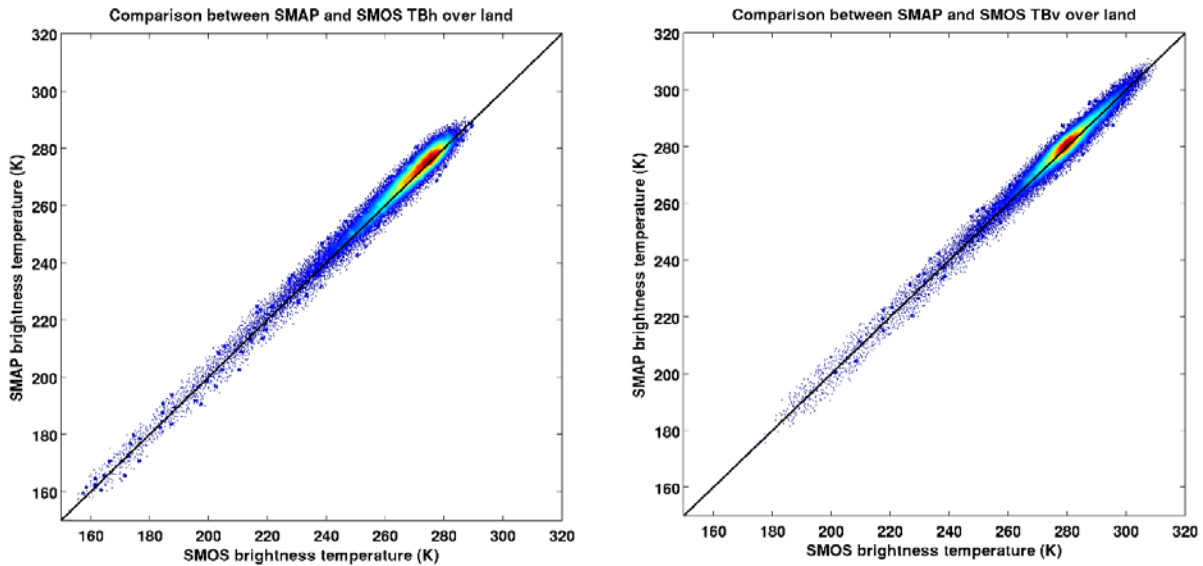


Figure 4.1. Density plot of the L1 brightness temperature comparison (top of the atmosphere) between SMAP (T15560) and SMOS (version 620) observations over land targets for V-pol (right) and H-pol (left).

the L1 radiometer error budget, the current single-look footprint NEDT of 1.1 K should result in an NEDT of less than 0.51 K on a 30 x 30 km grid. If all other error sources are within the requirements, this level of NEDT (< 0.51 K) should result in a total radiometric uncertainty of less than 1.3 K as required in the L2SMP error budget.

Table 4.2. Summary statistics of the brightness temperature comparison between SMOS (version 620) and SMAP (T15560) for May 5, 2015-March 31, 2018.

| | | RMSD (K) | R | Bias [SMAP-SMOS] (K) | ubRMSD (K) |
|-------|----------------|----------|--------|----------------------|------------|
| H pol | Land | 3.40 | 0.9921 | 1.15 | 3.20 |
| | Ocean | 2.44 | 0.7061 | 0.08 | 2.44 |
| | Overall | 2.71 | 0.9994 | 0.38 | 2.69 |
| V pol | Land | 3.05 | 0.9968 | 0.66 | 2.98 |
| | Ocean | 2.52 | 0.7679 | -0.23 | 2.51 |
| | Overall | 2.66 | 0.9994 | -0.02 | 2.66 |

4.1 Water Body Correction

Prior to implementing the actual soil moisture retrieval, a preliminary step in the processing is to perform a water body correction to the brightness temperature data for cases where a significant percentage of the grid cell contains open water. For the Version 6 L2SMP and Version 3 L2SMP_E, water correction is performed at the footprint level using the SMAP radiometer antenna gain pattern. This correction procedure is performed in the Version 4 SMAP L1B Radiometer Half-Orbit Time-Ordered Brightness Temperatures (L1BTB) product. Both the horizontally and vertically polarized L1B brightness temperatures over land are corrected for the presence of water within the antenna field of view (FOV). The resulting L1B brightness temperatures are then interpolated on the 36-km EASE Grid 2.0 projections using the inverse-distance squared interpolation method and on the 9-km EASE Grid 2.0 projections using the Backus-Gilbert optimal interpolation method. Overall it is expected that over land, the resulting brightness temperatures will become warmer upon the removal of the contribution of water to the original uncorrected observations. As stated in the product page of the Version 4 SMAP L1BTB product, water correction is performed as long as the antenna-gain-weighted water fraction within the antenna FOV is less than or equal to 0.9 and when the antenna boresight falls on a land location as indicated by a static high-resolution land/water mask. Further details of this procedure can be found in the User Guide, ATBD [13], or Assessment Report of the Version 4 SMAP L1B Radiometer Half-Orbit Time-Ordered Brightness Temperatures (L1BTB) product.

5 ALTERNATIVE L2SMP/L2SMP_E ALGORITHMS

The current L2SMP/L2SMP_E products contain soil moisture retrieval fields produced by the baseline and two optional algorithms. Inside an L2SMP/L2SMP_E granule the *soil_moisture* field is the one that links to the retrieval result produced by the currently-designated baseline algorithm. At present, the operational L2SMP/L2SMP_E Science Production Software (SPS) produces and stores soil moisture retrieval results from the following three algorithms:

1. Single Channel Algorithm V-pol (SCA-V)
2. Single Channel Algorithm H-pol (SCA-H)
3. Modified Dual Channel Algorithm (MDCA)

All algorithms operate on the same zeroth-order microwave emission model commonly known as the *tau-omega* model. In essence, this model relates brightness temperatures (SMAP L1 observations) to soil moisture (SMAP L2 retrievals) through ancillary information (e.g. soil texture, soil temperature, surface roughness, and vegetation water content) and a soil dielectric model. The algorithms differ in their approaches to solve for soil moisture from the model under different constraints and assumptions. Below is a concise description of these three algorithms. Further details are provided in [7].

Given the results to date from the L2SMP/L2SMP_E Cal/Val analyses, the SCA-V algorithm continues to deliver slightly better performance overall than the alternative algorithms. For this reason, the SCA-V will continue to be the operational baseline algorithm for this release of L2SMP/L2SMP_E data. Throughout the rest of the SMAP mission, the choice of the operational algorithm of the product will be evaluated on a regular basis as analyses of new observations and Cal/Val data become available or if significant improvements can be achieved by algorithm modifications.

5.1 Single Channel Algorithm V-pol (SCA-V)

In the SCA-V algorithm, the vertically polarized TB observations are converted to emissivity using a surrogate for the physical temperature of the emitting layer. The derived emissivity is corrected for vegetation and surface roughness to obtain the soil emissivity. The Fresnel equation is then used to determine the dielectric constant from the soil emissivity. Finally, a dielectric mixing model is used to solve for the soil moisture given knowledge of the soil texture. [Note: The software code includes the option of using different dielectric models. Currently, the software switch is set to the Mironov model [15]]. Analytically, SCA-V attempts to solve for one unknown variable (soil moisture) from one equation that relates the vertically polarized TB to soil moisture. Vegetation information is provided by an 11-year climatological data base of global NDVI and a table of *tau-omega* parameters based on land cover.

5.2 Single Channel Algorithm H-pol (SCA-H)

The SCA-H is similar to SCA-V in that the horizontally polarized TB observations are converted to emissivity using a surrogate for the physical temperature of the emitting layer. The derived emissivity is corrected for vegetation and surface roughness to obtain the soil emissivity. The Fresnel equation is then used to determine the dielectric constant. Finally, a dielectric mixing model is used to obtain the soil moisture given knowledge of the soil texture. Analytically, SCA-H attempts to solve for one unknown variable (soil moisture) from one equation that relates the horizontally polarized TB to soil moisture. Vegetation information is provided by an 11-year climatological data base of global NDVI and a table of *tau-omega* parameters based on land cover.

5.3 Modified Dual Channel Algorithm (MDCA)

The Modified Dual Channel Algorithm (MDCA) is an extension of the DCA described in previous assessment reports and replaces the DCA implemented in previous releases. In the MDCA, both the vertically and horizontally polarized TB observations are used to solve for soil moisture and vegetation optical depth. The algorithm iteratively minimizes a cost function (Φ^2) that consists of the sum of squares of the differences between the observed and estimated TBs:

$$\min \Phi_{\text{DCA}}^2 = (T_{\text{B,v}}^{\text{obs}} - T_{\text{B,v}}^{\text{est}})^2 + (T_{\text{B,h}}^{\text{obs}} - T_{\text{B,h}}^{\text{est}})^2 \quad (1)$$

In each iteration step, the soil moisture and vegetation opacity are adjusted simultaneously until the cost function attains a minimum in a least squares sense. Similar to SCA-V and SCA-H, ancillary information such as effective soil temperature, surface roughness, and vegetation single scattering albedo must be known *a priori* before the inversion process. MDCA permits polarization dependence of coefficients in the forward modeling of TB observations. As currently implemented for this release, the H and V parameters are set the same. In contrast with the SCA and the replaced DCA, the polarization mixing factor (Q) is assumed to be linearly related to the roughness parameter h by the equation $Q = 0.1771 h$ [19], and h is provided to the algorithm through a pre-computed static ancillary file with global values of h over the 3 km EASE-2 grid (see [7] for details). In addition to these differences, MDCA uses different values for the vegetation single scattering albedo.

5.4 Effective Temperature Methodology

In the June, 2018 data release, an improved depth correction scheme for the effective soil temperature was implemented. The use of an effective soil temperature is critical to accurate soil moisture retrieval. This effective soil temperature approach has been retained for the current release.

At L-band frequency, the contributing soil depth of microwave emission may be different from the pre-defined discrete soil depths at which the soil temperatures are available from a land surface model. The resulting discrepancy can contribute to a dry bias of retrieved soil moisture (i.e., retrieval lower than *in situ* soil moisture) if the model-based effective soil temperature is colder than the soil temperature "seen" by the radiometer. Conversely, wet bias of retrieved soil moisture will occur if the model-based effective soil temperature is warmer than the soil temperature "seen" by the radiometer. Since the contributing soil depth of microwave emission varies with soil moisture, the corresponding depth correction scheme for the effective soil temperature must account for soil moisture variability for brightness temperature observations acquired between AM (descending overpasses) and PM (ascending passes). To achieve this objective, the following modified formulation of the Choudhury model [16] has been found to result in good agreement between the *in situ* soil moisture data and the retrieved soil moisture:

$$T_{\text{eff}} = K \times [T_{\text{soil2}} + C (T_{\text{soil1}} - T_{\text{soil2}})]$$

where $C = 0.246$ for AM soil moisture retrieval and 1.000 for PM soil moisture retrieval, and $K = 1.000$ for IGBP land cover classes 1 through 5 (dense vegetation classes) and 1.020 elsewhere. T_{soil1} refers to the average soil temperature for the first soil layer (0-10 cm) and T_{soil2} refers to the average soil temperature for the second soil layer (10-20 cm) of the GMAO GEOS-5 land surface model.

6 METHODOLOGIES USED FOR L2SMP/L2SMP_E CAL/VAL

Validation is critical for accurate and credible product usage, and must be based on quantitative estimates of uncertainty. For satellite-based retrievals, validation should include direct comparison with independent correlative measurements. The assessment of uncertainty must also be conducted and presented to the community in normally used metrics in order to facilitate acceptance and implementation.

During mission definition and development, the SMAP Science Team and Cal/Val Working Group identified the metrics and methodologies that would be used for L2-L4 product assessment. These metrics and methodologies were vetted in community Cal/Val workshops and tested in SMAP pre-launch Cal/Val rehearsal campaigns. The methodologies identified and their general roles are:

- Core Validation Sites (CVS): Accurate estimates of products at matching scales for a limited set of conditions
- Sparse Networks: One point in the grid cell for a wide range of conditions
- Satellite Products: Estimates over a very wide range of conditions at matching scales
- Model Products: Estimates over a very wide range of conditions at matching scales
- Field Campaigns: Detailed estimates for a very limited set of conditions

In the case of the L2SMP/L2SMP_E data products, all of these methodologies can contribute to product assessment and improvement.

6.1 Validation Grid (VG)

The scanning radiometer on SMAP provides elliptical footprint observations across the scan. The orientation of this ellipse varies across the swath, and on successive passes a point on the ground might be observed with very different azimuth angles. A standard assumption in using radiometer observations is that the signal is dominated by the energy originating within the 3 dB (half-power) footprint (ellipse). The validity of this contributing area assumption will depend upon the heterogeneity of the landscape.

A major decision was made for SMAP to resample the radiometer data to an Earth-fixed grid at a resolution of 36 km. This was to facilitate temporal analyses and the disaggregation algorithm planned for the AP (active/passive) product. It ignores azimuth orientation and some contribution beyond the 3 dB footprints mentioned above, although the SMAP L1B_TB data do include a sidelobe correction. An important point is that TBs on the Earth-fixed 36-km grid are used in the retrieval of soil moisture, and it is the soil moisture for these 36-km grid cells that must be validated and improved.

The standard SMAP processor provides L2 surface (0-5 cm) soil moisture using only the radiometer (passive) data posted on a 36-km EASE2 Grid. The standard SMAP grid was established without any consideration of where the CVS might be located. In addition, the CVS were established in most cases to satisfy other (non-SMAP) objectives of the Cal/Val Partners. One of the criteria for categorizing a site as a CVS is that the number of individual *in situ* stations (N) within the site is large (target is $N \geq 9$ for 36 km). It was observed when examining the distribution of points at a site that in many cases only a few points fell in any specific standard 36-km grid cell. Therefore, it was decided that special SMAP validation grids (VGs) would be established for validation assessment that would be tied to the existing SMAP 3-km standard grid but would allow the shifting of the 36-km grids at a site to fully exploit N being as large as possible (i.e. the validation grid would be centered over the collection of *in situ* points at a given CVS to the extent possible). The approach used for validation grid processing is illustrated in Figure 6.1.

Validation Grid Processing Illustrated

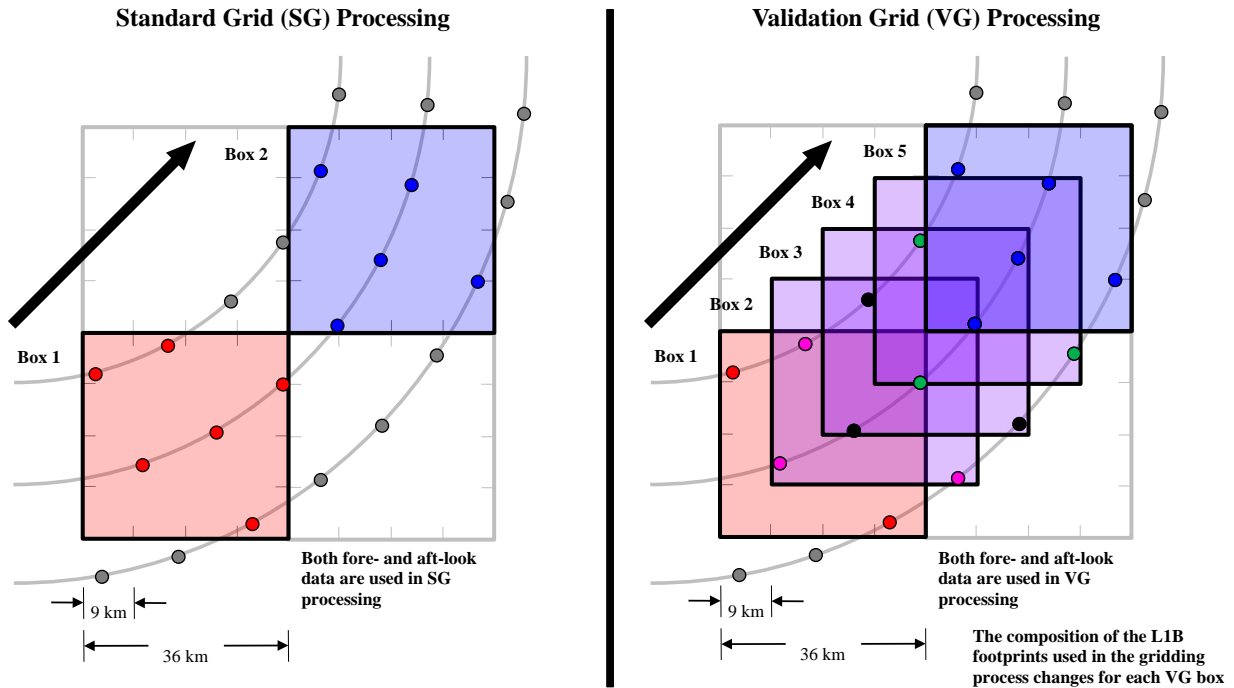


Figure 6.1. Illustration of validation grid processing. The EASE2 grid boxes are shifted by 3-km increments (although 9-km shifts are shown for clarity) to allow a better geographical match with the *in situ* validation sites.

Computationally the L2 and L3 VG products are the same as the standard product. The selection of the VGs for each site was done by members of the SMAP Algorithm Development Team and Science Team prelaunch. As noted, the 3-km grid does not change. The selection of the VGs also considered avoiding or minimizing the effects of land features that were not representative of the sampled domain or were known problems in retrieval (e.g., non-representative terrain, large water bodies, etc.).

7 SUMMARY OF REFINEMENTS IN L2SMP VERSION 6 AND L2SMP_E VERSION 3 AND VALIDATION

- *Expanded Assessment Period:* For the previous validated (Version 5) data release report, the analysis time period was April 1, 2015 – March 31, 2018 (36 months). The start date in 2015 was based on when the radiometer data were judged to be stable following instrument start-up operations. The end date was based upon the closing date of the Version 5 release report. The current assessment report expands the time period from April 1, 2015 through March 31, 2019, which provides a 4-year assessment.
- *New algorithm implementation:* MDCA was implemented as a replacement for the previous DCA. The MDCA achieves better retrieval performance through the modeling of polarization mixing between the vertically and horizontally polarized brightness temperature channels, as well as new estimates of single-scattering albedo and roughness coefficients.
- *Two previous optional algorithms dropped.* Previous optional algorithms MPRA (option 4) and E-DCA (option 5) were removed from this product release. These two optional algorithms are superseded by MDCA (option 3).
- *New output fields added.* A clay fraction field and a bulk density field were added to the Version 6 Standard 36 km Level 2 and Level 3 Radiometer Half-Orbit Soil Moisture Products and the Version 3 Enhanced 9 km Level 2 and Level 3 Radiometer Half-Orbit Soil Moisture Products to provide additional useful information to end users.

8 ASSESSMENTS

In this section several assessments and intercomparisons are presented. The standard L2SMP AM and PM (Version 6) and L2SMP_E AM and PM (Version 3) are examined for the expanded time period. Changes from the previous assessment (L2SMP Version 5 and L2SMP_E Version 2 [1]) will be noted if they occur. These assessments utilize CVS, sparse network, and SMOS comparisons.

8.1 L2SMP

8.1.1 Core Validation Sites

The primary validation for the L2SMP soil moisture is a comparison of retrievals at 36 km with ground-based observations that have been verified as providing a spatial average of soil moisture at the same scale, referred to as core validation sites (CVS) in the SMAP Calibration/Validation Plan [6].

In situ data are critical in the assessment of the SMAP products. These comparisons provide error estimates and a basis for modifying algorithms and/or parameters. A robust analysis will require many sites representing diverse conditions. However, there are relatively few sites that can provide the type and quality of data required. SMAP established a Cal/Val Partners Program in order to foster cooperation with these sites and to encourage the enhancement of these resources to better support SMAP Cal/Val. The current set of sites that provide data for L2SMP are listed in Table 8.1.

Not all of the sites in Table 8.1 have reached a level of maturity that would support their use as CVS. Prior to initiating the beta-release assessments, the L2SMP and Cal/Val Teams reviewed the status of all sites to determine which sites were ready to be designated as CVS. This process is repeated prior to each new assessment, with the addition of new screening procedures for *in situ* data as well as changes in upscaling at some CVS. The basic process is as follows:

- Develop and implement the validation grid
- Assess the site for conditions that would introduce uncertainty
- Determine if the number of points is large enough to provide reliable estimates
- Assess the geographic distribution of the *in situ* points
- Determine if the *in situ* instrumentation has been either (1) widely used and known to be well-calibrated or (2) calibrated for the specific site in question
- Perform quality assessment of each point in the network
- Establish a scaling function (default function is a linear average of all stations)
- Conduct pre-launch assessment using surrogate data appropriate for the SMAP L2SMP product (i.e. SMOS soil moisture)
- Review any supplemental studies that have been performed to verify that the network represents the SMAP product over the grid domain

The current CVS for the L2SMP product are marked with an asterisk in Table 8.1. A total of 15 CVS were used in this assessment. Each of these should have at least 9 points (ground *in situ* measurement stations); however, exceptions are made to allow fewer *in situ* stations if the site has a well-established scaling and calibration function. The status of candidate sites will continue to be reviewed periodically to determine if they should be classified as CVS and used in future assessments. Note that the table includes comments on sites that are used for some of the L2SMP_E analyses discussed later.

The *in situ* data downloaded from the Cal/Val Partners is run through an automatic quality control (QC) before determining the upscaled soil moisture values for each pixel (grid cell). The QC is implemented largely following the approach presented in [17]. The procedure includes checks for missing data, out of control values, spikes, sudden drops, and physical temperature limits. Additionally, the physical temperature is checked to be above 4°C because many sensors experience change in behavior at colder temperatures. In several cases the sites include stations that do not perform as expected, or at all, during the comparison period. These stations are removed from consideration altogether, and a new configuration is set for the site accounting for only the stations that produce a reasonable amount of data over the comparison period. Consequently, the upscaling functions for these sites are also based on the remaining set of stations.

The key tool used in L2SMP CVS analyses is illustrated by Figure 8.1. These charts are updated as changes are made to L1 data, L2 algorithms, or in preparation for periodic reviews with Cal/Val Partners. It includes a time series plot of *in situ* and retrieved soil moisture as well as flags that were triggered on a given day, an XY scatter plot of SMAP retrieved soil moisture compared to the average *in situ* soil moisture, and the quantitative statistical metrics. It also shows the CVS site distribution. When the *in situ* values are marked with a magenta color instead of red, it means that the *in situ* quality flag is raised. Several alternative algorithms and the SMOS soil moisture product are also displayed (SMOS L2 v650 was used). These plots are carefully reviewed and discussed by the L2SMP Team and Cal/Val Partners on a periodic basis. Systematic differences and anomalies are identified for further investigation.

All sites are then compiled to summarize the metrics and compute the overall performance. Tables 8.2 and 8.3 present the overall results for the current L2SMP Version 5 validated data sets. The combined scatter plots associated with these results are shown in Figure 8.2. These metrics and plots include the removal of questionable-quality and retrieval-flagged data.

The key results for this assessment are summarized in the SMAP Average results row in Table 8.2. First, all algorithms have about the same ubRMSE, differing by 0.009 m³/m³, and exceed or are very close to the SMAP mission goal of 0.040 m³/m³. Second, the correlations are also very similar. For both of these metrics, the SCA-V shows superior performance. More obvious differences among the algorithms were found in the bias, with the SCA-V now having an overall bias close to zero while the bias for the other algorithms is larger.

Based upon the metrics and considerations discussed, the SCA-V has been selected to continue as the operational baseline algorithm for this release (Version 6 L2SMP and Version 3 L2SMP_E). As a longer period of observations builds and additional CVS are added, the evaluations will be repeated on a periodic basis.

For guidance in expected performance, the SMOS soil moisture products for each site over the same time period were analyzed. Summary statistics are included in Table 8.2. For the CVS analyzed here, SMAP SCA-V outperforms SMOS for all metrics.

Also shown in Tables 8.2 and 8.3 are the metric averages from the L2SMP Version 4 and Version 5 assessments. As noted previously, in addition to the product changes, there is also a longer period of record associated with Version 6. Comparing the three versions, while the SCA algorithms appear to be stable over time, MDCA shows significant improvement with respect to DCA for all the statistical parameters and for both ascending and descending cases.

Table 8.1. SMAP Cal/Val Partner Sites Providing L2SMP Validation Data

| Site Name | Site PI | Area | Climate regime | IGBP Land Cover |
|-----------------|----------------|----------------|----------------|-------------------------|
| Walnut Gulch* | M. Cosh | USA (Arizona) | Arid | Shrub open |
| Reynolds Creek* | M. Cosh | USA (Idaho) | Arid | Grasslands |
| Fort Cobb* | M. Cosh | USA (Oklahoma) | Temperate | Grasslands |
| Little Washita* | M. Cosh | USA (Oklahoma) | Temperate | Grasslands |
| South Fork* | M. Cosh | USA (Iowa) | Cold | Croplands |
| Little River* | M. Cosh | USA (Georgia) | Temperate | Cropland/natural mosaic |
| TxSON* | T. Caldwell | USA (Texas) | Temperate | Grasslands |
| Millbrook | M. Temimi | USA (New York) | Cold | Deciduous broadleaf |
| Kenaston* | A. Berg | Canada | Cold | Croplands |
| Carman* | H. McNairn | Canada | Cold | Croplands |
| Monte Buey* | M. Thibeault | Argentina | Arid | Croplands |
| Bell Ville | M. Thibeault | Argentina | Arid | Croplands |
| REMEDHUS* | J. Martinez | Spain | Temperate | Croplands |
| Valencia | E. Lopez-Baeza | Spain | Arid | Woody Savannas |
| Twente* | Z. Su | Netherlands | Cold | Cropland/natural mosaic |
| HOBE* | F. Udall | Denmark | Temperate | Croplands |
| Kuwait | H. Jassar | Kuwait | Temperate | Barren/sparse |
| Niger | T. Pellarin | Niger | Arid | Grasslands |
| Benin | T. Pellarin | Benin | Arid | Savannas |
| Naqu | Z. Su | Tibet | Polar | Grasslands |
| Maqu | Z. Su | Tibet | Cold | Grasslands |
| Ngari | Z. Su | Tibet | Arid | Barren/sparse |
| MAHASRI* | J. Asanuma | Mongolia | Cold | Grasslands |
| Yanco* | J. Walker | Australia | Arid | Croplands |
| Kyeamba | J. Walker | Australia | Temperate | Croplands |

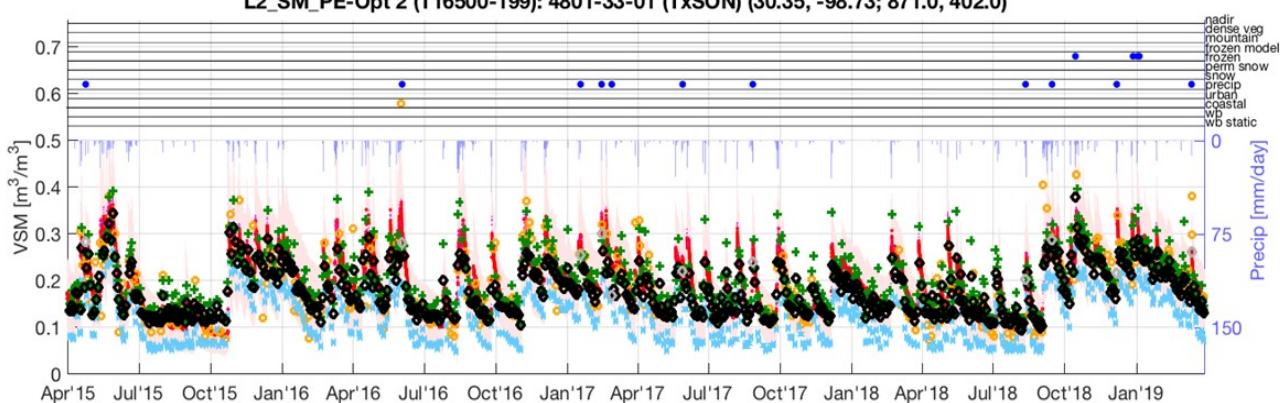
*=CVS used in both L2SMP and L2SMP_E assessments.

It should be noted that a small underestimation bias should be expected when comparing satellite retrievals to *in situ* soil moisture sensors during drying conditions. Satellite L-band microwave signals respond to a surface layer of a depth that varies with soil moisture (this depth is taken to be ~0-5 cm for average soils under average conditions). The *in situ* measurement is centered at 5 cm and measures a layer from ~ 3 to 7 cm. For some surface conditions and climates, it is expected that the surface will be slightly drier than the layer measured by the *in situ* sensors. For example, Adams et al. [18] reported that a mean difference of 0.018 m³/m³ existed between the measurements obtained by inserting a probe vertically from the surface versus horizontally at 5 cm for agricultural fields in Manitoba, Canada. Drier conditions were obtained using the surface measurement and this difference was more pronounced for mid- to dry conditions and minimized during wet conditions.

A review of the individual CVS indicates that several sites (South Fork, Little River, Carman, Fort Cobb and Twente) have larger bias values. Of these, South Fork, Carman and Twente also have large ubRMSE, which may suggest error sources that cannot be accounted for with the current algorithm/parameter approach. Efforts are under way at South Fork and Carman to better understand the causes of the errors and to determine if there is anything that can be done to mitigate these errors.

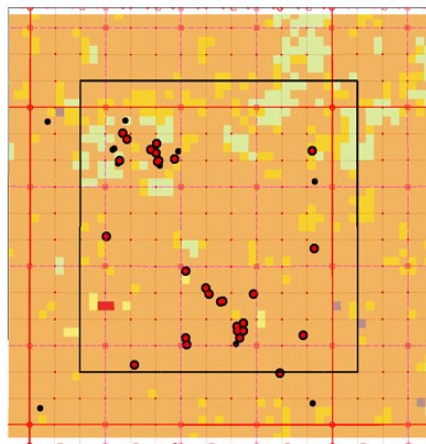
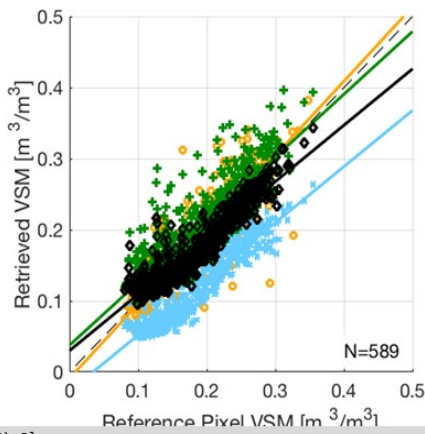
TxSON (Core Pixel)

L2_SM_PE-Opt 2 (T16500-199): 4801-33-01 (TxSON) (30.35, -98.73; 871.0, 402.0)



| Alg. | ubRMSE | Bias | RMSE | R | Slope |
|---------|--------|--------|-------|-------|-------|
| SCA-H | 0.021 | -0.066 | 0.069 | 0.935 | 0.790 |
| SCA-V | 0.021 | -0.008 | 0.023 | 0.934 | 0.793 |
| MDCA | 0.030 | 0.016 | 0.034 | 0.867 | 0.883 |
| SMOS | 0.043 | -0.000 | 0.043 | 0.842 | 1.044 |
| In Situ | | | | | |

Climate class: Temperate (Cfa)
Landcover: Grasslands
Soil texture:
S-%: 36
C-%: 31
BD: 1.43



Black: Use recommended [Retrieval Quality Flag bit(0)=0]
 Gray: Retrieval attempted and succeeded but use not recommended [bit(0)=1, bit(1)=0, bit(2)=0]
 Green: Retrieval attempted but failed [bit(0)=1, bit(1)=0, bit(2)=1]
 Cyan: Retrieval not attempted [bit(0)=1, bit(1)=1]

Not for public release or redistribution. This document has been reviewed and determined not to contain export controlled technical data.

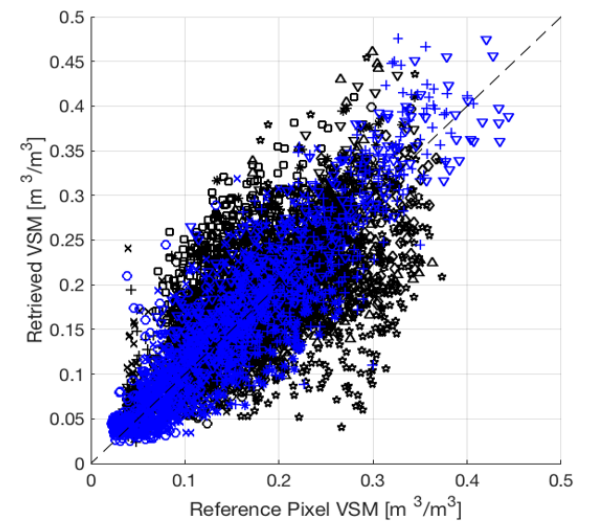
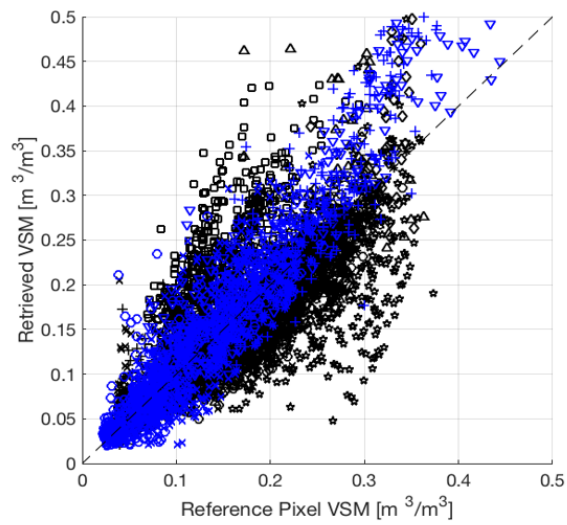
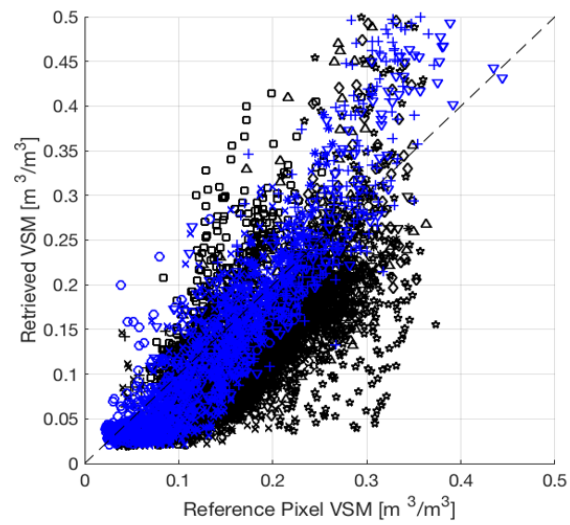
Figure 8.1. L2SMP assessment tool report for the TxSON core validation site descending (AM) passes.

Table 8.2. SMAP L2SMP Version 6 CVS Assessment for Descending (AM) Overpasses

| CVS | ubRMSE (m ³ /m ³) | | | Bias (m ³ /m ³) | | | RMSE (m ³ /m ³) | | | R | | | N | | |
|------------------------------|--|--------------|--------------|--|---------------|---------------|--|--------------|--------------|--------------|--------------|--------------|-------|-------|------|
| | SCA-H | SCA-V | MDCA | SCA-H | SCA-V | MDCA | SCA-H | SCA-V | MDCA | SCA-H | SCA-V | MDCA | SCA-H | SCA-V | MDCA |
| Reynolds Creek | 0.045 | 0.041 | 0.044 | -0.055 | -0.007 | 0.000 | 0.071 | 0.042 | 0.044 | 0.609 | 0.674 | 0.650 | 219 | 266 | 266 |
| Walnut Gulch | 0.025 | 0.025 | 0.029 | -0.020 | 0.009 | 0.015 | 0.031 | 0.027 | 0.033 | 0.759 | 0.812 | 0.805 | 360 | 474 | 475 |
| TxSON | 0.021 | 0.021 | 0.030 | -0.064 | -0.005 | 0.022 | 0.067 | 0.021 | 0.037 | 0.924 | 0.928 | 0.866 | 616 | 616 | 616 |
| Fort Cobb | 0.033 | 0.030 | 0.035 | -0.065 | -0.027 | -0.020 | 0.073 | 0.041 | 0.040 | 0.867 | 0.881 | 0.846 | 618 | 619 | 619 |
| Little Washita | 0.023 | 0.021 | 0.032 | -0.057 | -0.013 | 0.005 | 0.062 | 0.025 | 0.032 | 0.900 | 0.924 | 0.862 | 652 | 652 | 651 |
| South Fork | 0.062 | 0.053 | 0.052 | -0.034 | -0.009 | -0.021 | 0.071 | 0.054 | 0.056 | 0.594 | 0.642 | 0.623 | 349 | 355 | 355 |
| Little River | 0.047 | 0.036 | 0.036 | 0.040 | 0.089 | 0.082 | 0.062 | 0.096 | 0.090 | 0.770 | 0.794 | 0.739 | 482 | 484 | 485 |
| Kenaston | 0.037 | 0.027 | 0.036 | -0.058 | -0.025 | -0.011 | 0.069 | 0.037 | 0.038 | 0.770 | 0.827 | 0.671 | 235 | 235 | 235 |
| Carman | 0.098 | 0.069 | 0.067 | -0.073 | -0.066 | -0.078 | 0.123 | 0.096 | 0.103 | 0.516 | 0.563 | 0.510 | 317 | 318 | 320 |
| Monte Buey | 0.071 | 0.049 | 0.040 | -0.033 | -0.014 | -0.034 | 0.078 | 0.051 | 0.053 | 0.760 | 0.879 | 0.745 | 176 | 189 | 193 |
| REMEDHUS | 0.042 | 0.040 | 0.040 | -0.020 | 0.005 | 0.006 | 0.046 | 0.041 | 0.040 | 0.852 | 0.847 | 0.829 | 499 | 511 | 511 |
| Twente | 0.072 | 0.054 | 0.049 | 0.023 | 0.045 | -0.001 | 0.076 | 0.071 | 0.049 | 0.879 | 0.889 | 0.851 | 330 | 347 | 348 |
| HOBE | 0.046 | 0.029 | 0.025 | 0.019 | -0.007 | -0.065 | 0.050 | 0.030 | 0.070 | 0.867 | 0.876 | 0.757 | 58 | 58 | 58 |
| MAHASRI | 0.031 | 0.030 | 0.030 | 0.000 | 0.006 | 0.009 | 0.031 | 0.031 | 0.032 | 0.825 | 0.854 | 0.845 | 315 | 293 | 318 |
| Yanco | 0.043 | 0.037 | 0.035 | 0.001 | 0.032 | 0.024 | 0.043 | 0.050 | 0.042 | 0.941 | 0.947 | 0.933 | 337 | 342 | 348 |
| Mean Absolute Bias | | | | 0.038 | 0.024 | 0.026 | | | | | | | | | |
| SMAP L2SMP Average V6 | 0.046 | 0.038 | 0.039 | -0.026 | 0.001 | -0.005 | 0.063 | 0.047 | 0.051 | 0.789 | 0.822 | 0.769 | | | |
| SMAP L2SMP Average V5 | 0.046 | 0.037 | 0.047 | -0.028 | -0.001 | 0.038 | 0.062 | 0.044 | 0.070 | 0.788 | 0.821 | 0.737 | | | |
| SMOS L2SM Average V5 | 0.053 | | | -0.024 (MAB=0.035) | | | 0.065 | | | 0.671 | | | | | |
| SMAP L2SMP Average V4 | 0.046 | 0.039 | 0.047 | -0.037 | -0.028 | -0.015 | 0.071 | 0.061 | 0.066 | 0.772 | 0.795 | 0.700 | | | |
| SMOS L2SMP Average V4 | 0.053 | | | -0.028 | | | 0.072 | | | 0.710 | | | | | |

Table 8.3. SMAP L2SMP Version 6 CVS Assessment for Ascending (PM) Overpasses

| CVS | ubRMSE (m ³ /m ³) | | | Bias (m ³ /m ³) | | | RMSE (m ³ /m ³) | | | R | | | N | | |
|------------------------------|--|--------------|--------------|--|---------------|---------------|--|--------------|--------------|---------------|--------------|--------------|-------|-------|------|
| | SCA-H | SCA-V | MDCA | SCA-H | SCA-V | MDCA | SCA-H | SCA-V | MDCA | SCA-H | SCA-V | MDCA | SCA-H | SCA-V | MDCA |
| Reynolds Creek | 0.047 | 0.042 | 0.042 | -0.062 | -0.013 | -0.003 | 0.078 | 0.044 | 0.043 | 0.607 | 0.696 | 0.695 | 251 | 307 | 307 |
| Walnut Gulch | 0.026 | 0.026 | 0.030 | -0.032 | -0.001 | 0.005 | 0.041 | 0.026 | 0.030 | 0.709 | 0.746 | 0.740 | 504 | 677 | 680 |
| TxSON | 0.019 | 0.019 | 0.028 | -0.055 | -0.001 | 0.016 | 0.058 | 0.019 | 0.032 | 0.930 | 0.931 | 0.856 | 649 | 649 | 649 |
| Fort Cobb | 0.038 | 0.030 | 0.030 | -0.061 | -0.031 | -0.031 | 0.072 | 0.043 | 0.043 | 0.872 | 0.885 | 0.853 | 662 | 663 | 663 |
| Little Washita | 0.025 | 0.022 | 0.030 | -0.046 | -0.008 | -0.001 | 0.052 | 0.023 | 0.030 | 0.898 | 0.917 | 0.836 | 676 | 676 | 674 |
| South Fork | 0.061 | 0.045 | 0.051 | -0.032 | -0.017 | -0.027 | 0.068 | 0.048 | 0.058 | 0.623 | 0.731 | 0.672 | 375 | 378 | 378 |
| Little River | 0.045 | 0.035 | 0.040 | 0.049 | 0.091 | 0.078 | 0.066 | 0.098 | 0.088 | 0.777 | 0.762 | 0.597 | 407 | 407 | 407 |
| Kenaston | 0.036 | 0.024 | 0.041 | -0.051 | -0.023 | -0.015 | 0.062 | 0.033 | 0.044 | 0.809 | 0.871 | 0.650 | 301 | 301 | 301 |
| Carman | 0.088 | 0.056 | 0.056 | -0.070 | -0.069 | -0.087 | 0.113 | 0.089 | 0.103 | 0.529 | 0.634 | 0.560 | 288 | 291 | 291 |
| Monte Buey | 0.065 | 0.041 | 0.040 | -0.006 | -0.005 | -0.042 | 0.065 | 0.041 | 0.058 | 0.855 | 0.910 | 0.701 | 178 | 192 | 196 |
| REMEDHUS | 0.043 | 0.040 | 0.041 | -0.030 | -0.005 | -0.004 | 0.052 | 0.041 | 0.041 | 0.820 | 0.818 | 0.797 | 548 | 577 | 579 |
| Twente | 0.073 | 0.052 | 0.043 | 0.043 | 0.050 | -0.008 | 0.085 | 0.072 | 0.044 | 0.894 | 0.910 | 0.876 | 417 | 436 | 441 |
| HOBE | 0.041 | 0.026 | 0.027 | 0.031 | 0.004 | -0.058 | 0.051 | 0.026 | 0.064 | 0.842 | 0.821 | 0.630 | 58 | 58 | 58 |
| MAHASRI | 0.031 | 0.031 | 0.032 | -0.010 | 0.000 | 0.000 | 0.033 | 0.031 | 0.032 | 0.760 | 0.757 | 0.747 | 427 | 423 | 452 |
| Yanco | 0.052 | 0.04 | 0.032 | 0.010 | 0.033 | 0.018 | 0.053 | 0.052 | 0.037 | 0.949 | 0.954 | 0.940 | 380 | 384 | 389 |
| Mean Absolute Bias | | | | 0.039 | 0.023 | 0.026 | | | | | | | | | |
| SMAP L2SMP Average V6 | 0.046 | 0.035 | 0.038 | -0.022 | 0.000 | -0.011 | 0.063 | 0.046 | 0.050 | 0.0791 | 0.823 | 0.743 | | | |
| SMAP L2SMP Average V5 | 0.045 | 0.035 | 0.045 | -0.023 | -0.002 | 0.030 | 0.062 | 0.044 | 0.064 | 0.791 | 0.821 | 0.724 | | | |
| SMOS L2SMP Average V5 | 0.051 | | | -0.031 (MAB=0.036) | | | 0.066 | | | 0.686 | | | | | |
| SMAP L2SMP Average V4 | 0.046 | 0.039 | 0.047 | -0.037 | -0.028 | -0.015 | 0.071 | 0.061 | 0.066 | 0.772 | 0.795 | 0.700 | | | |
| SMOS L2SMP Average V4 | 0.053 | | | -0.028 | | | 0.072 | | | 0.710 | | | | | |



- x Reynolds Creek (04013601)
- + Walnut Gulch (16013601)
- * TxSON (48013601)
- o Fort Cobb (16033601)
- ∇ Little Washita (16023601)
- △ South Fork (16073601)
- Little River (16043605)
- ☆ Kenaston (27013601)
- ★ Carman (09013611)
- ◇ Monte Buey (19023601)
- x REMEDHUS (03013602)
- + Twente (12043606)
- * HOBE (67013601)
- o MAHASRI (53013601)
- ∇ Yanco (07013601)

Figure 8.2. Scatterplot of SMAP L2SMP Version 65 CVS Assessment for Descending (AM) Overpasses (SCA-H left panel, SCA-V middle panel, and MDCA right panel).

8.1.2 Sparse Networks

The intensive network CVS validation described above can be complemented by sparse networks as well as by new/emerging types of soil moisture networks. The current set of networks being utilized by SMAP are listed in Table 8.4.

The defining feature of these networks is that the measurement density is low, usually resulting in one ground measurement point per SMAP footprint. These observations cannot be used for validation without addressing two issues: verifying that they provide a reliable estimate of the 0-5 cm surface soil moisture layer and that the one measurement point is representative of conditions across the entire SMAP footprint.

SMAP has been evaluating methodologies for upscaling data from these networks to SMAP footprint resolutions. A key element of the upscaling approach is Triple Collocation that combines the *in situ* data and SMAP soil moisture product with another independent source of soil moisture, likely to be a model-based product [5].

Although limited by upscaling, sparse networks do offer many sites in different environments and are typically operational with very low latency. They are very useful as a supplement to the limited number of CVS.

Table 8.4. Sparse Networks Providing L2SMP and L2SMP_E Validation Data

| Network Name | PI/Contact | Area | No. of Sites (L2SMP) | No. of Sites (L2SMP_E) |
|--|--------------|-----------------|----------------------|------------------------|
| NOAA Climate Reference Network (CRN) | M. Palecki | USA | 60 | 56 |
| USDA NRCS Soil Climate Analysis Network (SCAN) | M. Cosh | USA | 101 | 100 |
| GPS | E. Small | Western USA | 80 | 77 |
| COSMOS | M. Zreda | Mostly USA | 30 | 32 |
| SMOSMania | J. Calvet | Southern France | 10 | 11 |
| Pampas | M. Thibeault | Argentina | 16 | 14 |
| Oklahoma Mesonet | - | Oklahoma, USA | 94 | 96 |
| Mongolian Grasslands (MAHASRI) | J. Asanuma | Mongolia | 13 | 13 |

The sparse network metrics are summarized in Table 8.5 and 8.6. Because of the larger number of sites, it is possible to also examine the results based upon the IGBP land cover classification used by SMAP. For these comparisons the SMOS metrics are included for each category. The reliability of the analyses based upon these classes will depend upon the number of sites available (N).

Overall, the relative performance of the algorithms based on ubRMSE is similar to that obtained from the CVS -- SCA-V has the best metrics, with an ubRMSE of 0.049 m³/m³, bias of 0.006 m³/m³ and correlation of 0.663 for AM orbits, and an ubRMSE of 0.050 m³/m³, bias of 0.009 m³/m³ and correlation of 0.637 for the PM orbits. Compared to the CVS results, the sparse network values are higher for ubRMSE and bias and lower for R, which is expected due to the significant change in scale between a point and the grid product. When comparing Version 6 to Version 5 and Version 4, SCA-V exhibits steady improvements over performance metrics; similarly, MDCA is a significant improvement over the earlier DCA. Considering the many caveats that must be considered in making sparse network comparisons, the algorithm performance is quite good. This result provides additional confidence in the previous conclusions based on the CVS.

Interpreting the results based on land cover is more complex. There are no clear patterns associated with broader vegetation types. The ubRMSE values for SCA-V are all between 0.028 and 0.069 m^3/m^3 . Grasslands had larger bias values, which needs to be investigated. Forest results are based on very limited sites and should not be generalized.

Figure 8.3 contains scatterplots of the SCA-V retrieved versus observed *in situ* soil moisture for SMAP standard and enhanced L2 passive soil moisture products from the previous release. The equivalent scatter plots from the current release (V6 L2SMP and V3 L2SMP_E) are very similar to Fig. 8.3 and reflect the summary metrics discussed above.

SMOS (Level 2 UDP) metrics are also included in Tables 8.5 and 8.6 (in blue) as supporting information. It should be noted that while SMOS retrievals are based on a different land cover classification scheme (ECOCLIMAP), this does not have any impact on the comparisons shown, which compares the soil moisture retrievals to the *in situ* observations for the points that fall into these categories. Overall, the SMOS products are showing a higher bias and ubRMSE and lower correlation than the SMAP SCA-V retrievals. There was a small increase in ubRMSE and decrease in bias in the SMOS results compared to the Version 5 analysis.

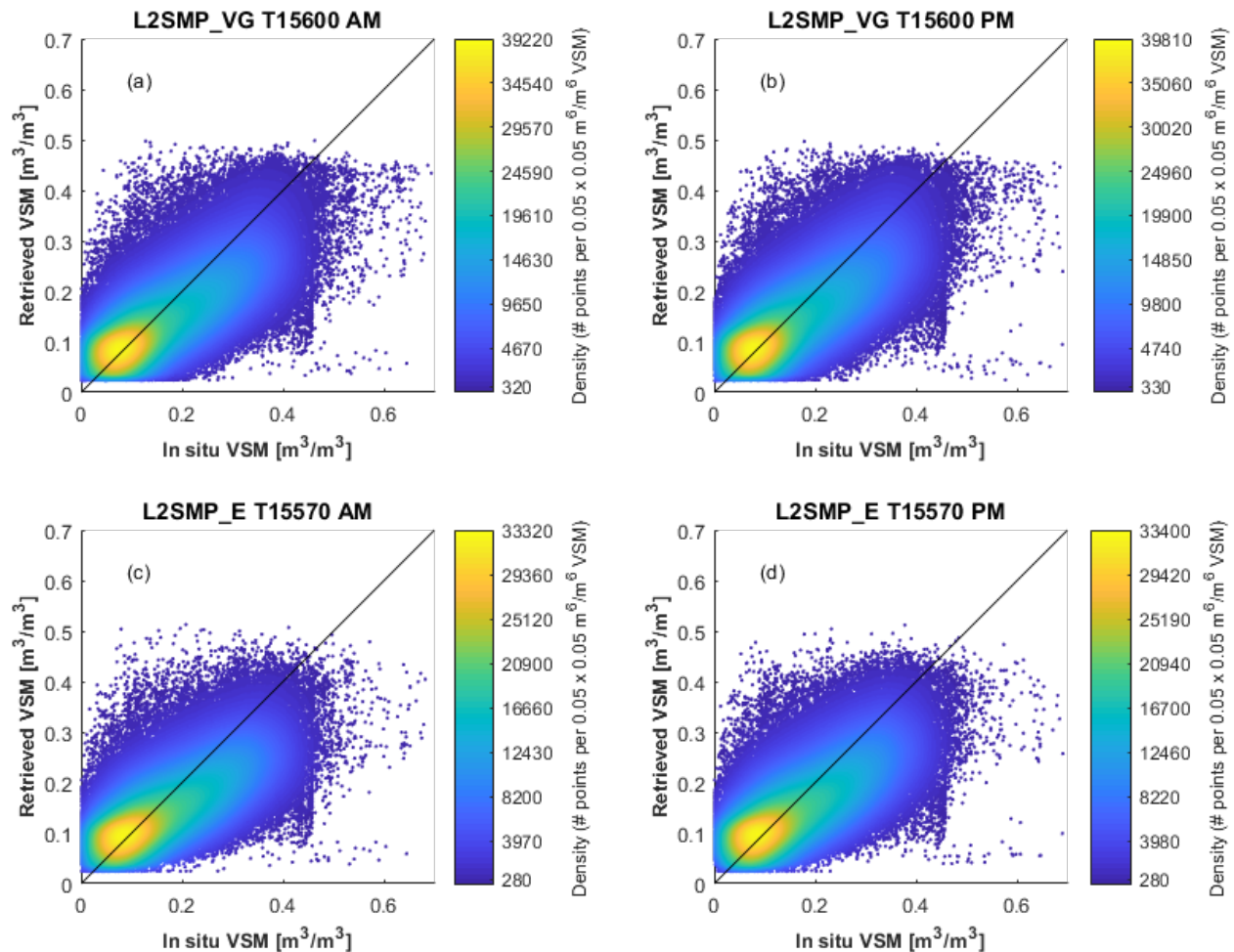


Figure 8.3. Scatterplots of the sparse network *in situ* observations and SMAP baseline SCA-V retrievals: (a) L2SMP AM Version 5, (b) L2SMP PM Version 5, (c) L2SMP_E AM Version 2, and (d) L2SMP_E PM Version 2.

Table 8.5. SMAP L2SMP Version 6 Sparse Network Assessment for Descending (AM) Overpasses

| IGBP Class | ubRMSD (m ³ /m ³) | | | | Bias (m ³ /m ³) | | | | RMSD (m ³ /m ³) | | | | R | | | | N |
|---|--|--------------|--------------|--------------|--|---------------|--------------|---------------|--|--------------|--------------|--------------|--------------|--------------|--------------|--------------|-----|
| | SCA-H | SCA-V | MDCA | SMOS | SCA-H | SCA-V | MDCA | SMOS | SCA-H | SCA-V | MDCA | SMOS | SCA-H | SCA-V | MDCA | SMOS | |
| Evergreen needleleaf forest | 0.040 | 0.037 | 0.040 | 0.069 | -0.059 | -0.007 | 0.012 | -0.060 | 0.072 | 0.038 | 0.045 | 0.095 | 0.822 | 0.836 | 0.794 | 0.511 | 3 |
| Evergreen broadleaf forest | | | | | | | | | | | | | | | | | |
| Deciduous needleleaf forest | | | | | | | | | | | | | | | | | |
| Deciduous broadleaf forest | | | | | | | | | | | | | | | | | |
| Mixed forest | 0.045 | 0.044 | 0.049 | 0.084 | -0.042 | 0.013 | 0.022 | -0.081 | 0.062 | 0.051 | 0.062 | 0.117 | 0.661 | 0.666 | 0.603 | 0.627 | 2 |
| Closed shrublands | | | | | | | | | | | | | | | | | |
| Open shrublands | 0.039 | 0.039 | 0.044 | 0.051 | -0.037 | 0.004 | 0.022 | -0.005 | 0.055 | 0.062 | 0.077 | 0.062 | 0.587 | 0.598 | 0.586 | 0.548 | 41 |
| Woody savannas | 0.062 | 0.058 | 0.065 | 0.097 | -0.040 | 0.011 | 0.009 | -0.064 | 0.088 | 0.090 | 0.134 | 0.140 | 0.687 | 0.708 | 0.624 | 0.491 | 20 |
| Savannas | 0.046 | 0.045 | 0.047 | 0.057 | -0.038 | 0.003 | 0.002 | -0.021 | 0.061 | 0.062 | 0.081 | 0.070 | 0.88 | 0.872 | 0.852 | 0.824 | 6 |
| Grasslands | 0.051 | 0.050 | 0.053 | 0.061 | -0.067 | -0.025 | -0.010 | -0.046 | 0.070 | 0.071 | 0.084 | 0.087 | 0.678 | 0.69 | 0.661 | 0.612 | 226 |
| Permanent wetlands | 0.081 | 0.069 | 0.066 | 0.096 | -0.005 | 0.017 | 0.027 | -0.042 | 0.071 | 0.071 | 0.085 | 0.105 | 0.388 | 0.396 | 0.324 | 0.392 | 1 |
| Croplands | 0.078 | 0.067 | 0.067 | 0.082 | -0.033 | -0.007 | -0.007 | -0.041 | 0.097 | 0.098 | 0.106 | 0.120 | 0.547 | 0.594 | 0.554 | 0.545 | 59 |
| Urban and built-up | | | | | | | | | | | | | | | | | |
| Crop/Natural vegetation mosaic | 0.063 | 0.057 | 0.061 | 0.092 | -0.007 | 0.037 | 0.029 | -0.052 | 0.085 | 0.087 | 0.087 | 0.138 | 0.646 | 0.694 | 0.654 | 0.441 | 15 |
| Snow and ice | | | | | | | | | | | | | | | | | |
| Barren/Sparse | 0.027 | 0.028 | 0.031 | 0.043 | -0.018 | 0.012 | 0.025 | -0.004 | 0.042 | 0.046 | 0.053 | 0.051 | 0.587 | 0.576 | 0.557 | 0.513 | 6 |
| Mean Absolute Bias | | | | | 0.064 | 0.055 | 0.059 | 0.081 | | | | | | | | | |
| SMAP L2SMP Average V6 | 0.053 | 0.049 | 0.052 | 0.073 | -0.035 | 0.006 | 0.013 | -0.042 | 0.077 | 0.066 | 0.070 | 0.099 | 0.648 | 0.663 | 0.621 | 0.550 | |
| SMAP L2SMP Average V5 | 0.055 | 0.049 | 0.059 | 0.072 | -0.035 | 0.004 | 0.063 | -0.049 | 0.078 | 0.066 | 0.099 | 0.102 | 0.623 | 0.664 | 0.573 | 0.559 | |
| SMAP L2SMP Average V4 | 0.053 | 0.050 | 0.057 | 0.066 | -0.061 | -0.031 | 0.010 | -0.049 | 0.093 | 0.077 | 0.081 | 0.099 | 0.643 | 0.663 | 0.633 | 0.576 | |
| Average is based upon all sets of observations, not the average of the land cover category results. | | | | | | | | | | | | | | | | | |

Table 8.6. SMAP L2SMP Version 6 Sparse Network Assessment for Ascending (PM) Overpasses

| IGBP Class | ubRMSD (m ³ /m ³) | | | | Bias (m ³ /m ³) | | | | RMSD (m ³ /m ³) | | | | R | | | | N |
|--------------------------------|--|--------------|--------------|--------------|--|---------------|---------------|---------------|--|--------------|--------------|--------------|--------------|--------------|--------------|--------------|-----|
| | SCA-H | SCA-V | MDCA | SMOS | SCA-H | SCA-V | MDCA | SMOS | SCA-H | SCA-V | MDCA | SMOS | SCA-H | SCA-V | MDCA | SMOS | |
| Evergreen needleleaf forest | 0.042 | 0.039 | 0.043 | 0.061 | -0.053 | -0.002 | 0.015 | -0.042 | 0.068 | 0.040 | 0.048 | 0.076 | 0.770 | 0.784 | 0.741 | 0.624 | 3 |
| Evergreen broadleaf forest | | | | | | | | | | | | | | | | | |
| Deciduous needleleaf forest | | | | | | | | | | | | | | | | | |
| Deciduous broadleaf forest | | | | | | | | | | | | | | | | | |
| Mixed forest | 0.048 | 0.045 | 0.051 | 0.091 | -0.040 | 0.012 | 0.019 | -0.029 | 0.062 | 0.049 | 0.060 | 0.096 | 0.590 | 0.599 | 0.503 | 0.578 | 2 |
| Closed shrublands | | | | | | | | | | | | | | | | | |
| Open shrublands | 0.039 | 0.039 | 0.044 | 0.052 | -0.042 | 0.001 | 0.019 | -0.006 | 0.063 | 0.054 | 0.060 | 0.066 | 0.561 | 0.559 | 0.545 | 0.503 | 41 |
| Woody savannas | 0.063 | 0.058 | 0.065 | 0.096 | -0.019 | 0.023 | 0.009 | -0.051 | 0.094 | 0.090 | 0.089 | 0.131 | 0.688 | 0.703 | 0.603 | 0.515 | 20 |
| Savannas | 0.047 | 0.047 | 0.051 | 0.056 | -0.034 | 0.007 | 0.006 | -0.031 | 0.070 | 0.063 | 0.067 | 0.077 | 0.869 | 0.854 | 0.823 | 0.828 | 6 |
| Grasslands | 0.051 | 0.049 | 0.052 | 0.06 | -0.063 | -0.024 | -0.012 | -0.041 | 0.088 | 0.069 | 0.072 | 0.085 | 0.683 | 0.691 | 0.654 | 0.623 | 226 |
| Permanent wetlands | 0.082 | 0.066 | 0.062 | 0.085 | 0.004 | 0.012 | 0.004 | -0.059 | 0.082 | 0.067 | 0.062 | 0.103 | 0.389 | 0.415 | 0.354 | 0.432 | 1 |
| Croplands | 0.077 | 0.065 | 0.065 | 0.079 | -0.017 | 0.000 | -0.012 | -0.039 | 0.110 | 0.096 | 0.097 | 0.113 | 0.552 | 0.602 | 0.548 | 0.546 | 59 |
| Urban and built-up | | | | | | | | | | | | | | | | | |
| Crop/Natural vegetation mosaic | 0.063 | 0.057 | 0.063 | 0.090 | 0.015 | 0.05 | 0.031 | -0.049 | 0.083 | 0.091 | 0.090 | 0.129 | 0.648 | 0.687 | 0.610 | 0.430 | 15 |
| Snow and ice | | | | | | | | | | | | | | | | | |
| Barren/Sparse | 0.028 | 0.029 | 0.033 | 0.046 | -0.020 | 0.013 | 0.026 | 0.005 | 0.043 | 0.047 | 0.054 | 0.054 | 0.519 | 0.477 | 0.440 | 0.387 | 6 |
| Mean Absolute Bias | | | | | 0.063 | 0.056 | 0.058 | 0.076 | | | | | | | | | |
| SMAP L2SMP Average V6 | 0.054 | 0.050 | 0.053 | 0.072 | -0.027 | 0.009 | 0.011 | -0.034 | 0.076 | 0.067 | 0.070 | 0.093 | 0.627 | 0.637 | 0.582 | 0.547 | |
| SMAP L2SMP Average V5 | 0.056 | 0.049 | 0.060 | 0.070 | -0.026 | 0.008 | 0.061 | -0.041 | 0.077 | 0.067 | 0.099 | 0.096 | 0.606 | 0.637 | 0.522 | 0.561 | |
| SMAP L2SMP Average V4 | 0.053 | 0.051 | 0.059 | 0.065 | -0.063 | -0.043 | -0.016 | -0.043 | 0.097 | 0.083 | 0.084 | 0.095 | 0.618 | 0.629 | 0.595 | 0.578 | |

Average is based upon all sets of observations, not the average of the land cover category results.

8.2 L2SMP_E

8.2.1 Core Validation Sites

The new L2SMP_E Version 3 is assessed using the same approach as that employed for L2SMP. The major difference between L2SMP_E and L2SMP is that this product is assessed using a different set of CVS. Because it is possible to now provide a retrieval for every SMAP 9-km grid cell where feasible, the need for using the validation grid (as used for L2SMP) is not expected to be as important an issue in performing validation. It should be noted that the validation grid allowed centering the retrieval on any 3-km grid, whereas the L2SMP_E retrieval process can only be centered on a 9-km grid. Thus, the ability to match the *in situ* network to the grid may be more restrictive for L2SMP_E. Each available CVS was reviewed to identify the 9-km grid cell that satisfied the CVS criteria for the new 33-km contributing domain. Therefore, the mix/weighting of *in situ* stations and grid center will be different between the CVS sets used for the two products.

The CVS results are summarized in Tables 8.7 and 8.8 for the AM and PM overpasses, respectively. The best algorithm choice remains the SCA-V and the ubRMSE meets/exceeds the SMAP mission requirements. When compared to the L2SMP retrievals, the differences in the metrics are negligible. These results indicate that the L2SMP_E products can be used in place of L2SMP without loss of accuracy.

8.2.2 Sparse Networks

The sparse network results are summarized in Tables 8.9 and 8.10 for the AM and PM overpasses, respectively. Comparing the overall metrics for the L2SMP products to the L2SMP_E products, the results are nearly identical and therefore support the trends observed in the CVS analysis.

Table 8.7. SMAP L2SMP_E Version 3 CVS Assessment for Descending (AM) Overpasses

| CVS | ubRMSE (m ³ /m ³) | | | Bias (m ³ /m ³) | | | RMSE (m ³ /m ³) | | | R | | | N | | |
|--------------------------------|--|--------------|--------------|--|---------------|---------------|--|--------------|--------------|--------------|--------------|--------------|-------|-------|------|
| | SCA-H | SCA-V | MDCA | SCA-H | SCA-V | MDCA | SCA-H | SCA-V | MDCA | SCA-H | SCA-V | MDCA | SCA-H | SCA-V | MDCA |
| Reynolds Creek | 0.040 | 0.040 | 0.045 | -0.059 | -0.013 | -0.002 | 0.071 | 0.042 | 0.046 | 0.639 | 0.653 | 0.046 | 141 | 147 | 147 |
| Walnut Gulch | 0.024 | 0.026 | 0.029 | -0.016 | 0.015 | 0.022 | 0.029 | 0.030 | 0.036 | 0.767 | 0.796 | 0.036 | 198 | 238 | 238 |
| TxSON | 0.021 | 0.021 | 0.030 | -0.066 | -0.008 | 0.016 | 0.069 | 0.023 | 0.034 | 0.935 | 0.934 | 0.034 | 589 | 589 | 589 |
| Fort Cobb | 0.033 | 0.029 | 0.034 | -0.083 | -0.047 | -0.04 | 0.089 | 0.055 | 0.052 | 0.864 | 0.878 | 0.052 | 518 | 518 | 518 |
| Little Washita | 0.023 | 0.021 | 0.032 | -0.062 | -0.018 | -0.001 | 0.066 | 0.028 | 0.032 | 0.894 | 0.912 | 0.032 | 487 | 487 | 487 |
| South Fork | 0.059 | 0.052 | 0.053 | -0.056 | -0.038 | -0.057 | 0.081 | 0.064 | 0.078 | 0.694 | 0.705 | 0.078 | 340 | 347 | 347 |
| Little River | 0.045 | 0.036 | 0.036 | 0.012 | 0.059 | 0.051 | 0.046 | 0.069 | 0.063 | 0.756 | 0.783 | 0.063 | 501 | 501 | 502 |
| Kenaston | 0.042 | 0.031 | 0.035 | -0.026 | 0.007 | 0.020 | 0.050 | 0.031 | 0.040 | 0.717 | 0.774 | 0.040 | 262 | 262 | 262 |
| Carman | 0.089 | 0.067 | 0.061 | -0.061 | -0.050 | -0.061 | 0.108 | 0.083 | 0.086 | 0.531 | 0.587 | 0.086 | 317 | 321 | 322 |
| Monte Buey | 0.075 | 0.051 | 0.038 | -0.033 | -0.015 | -0.039 | 0.082 | 0.053 | 0.054 | 0.748 | 0.860 | 0.054 | 219 | 236 | 247 |
| REMEDHUS | 0.044 | 0.042 | 0.041 | -0.011 | 0.017 | 0.016 | 0.045 | 0.045 | 0.044 | 0.845 | 0.845 | 0.044 | 463 | 469 | 469 |
| Twente | 0.072 | 0.054 | 0.049 | 0.023 | 0.045 | -0.001 | 0.076 | 0.071 | 0.049 | 0.879 | 0.889 | 0.049 | 330 | 347 | 348 |
| HOBE | 0.049 | 0.036 | 0.051 | 0.004 | -0.003 | -0.046 | 0.049 | 0.036 | 0.069 | 0.723 | 0.860 | 0.069 | 117 | 117 | 117 |
| MAHASRI | 0.031 | 0.030 | 0.030 | 0.000 | 0.006 | 0.009 | 0.031 | 0.031 | 0.032 | 0.825 | 0.854 | 0.032 | 315 | 293 | 318 |
| Yanco | 0.044 | 0.039 | 0.038 | -0.018 | 0.014 | 0.008 | 0.047 | 0.041 | 0.039 | 0.921 | 0.932 | 0.039 | 391 | 396 | 402 |
| Mean Absolute Bias | | | | 0.035 | 0.024 | 0.026 | | | | | | | | | |
| SMAP L2SMP_E Average V3 | 0.046 | 0.038 | 0.040 | -0.030 | -0.002 | -0.007 | 0.063 | 0.047 | 0.050 | 0.783 | 0.817 | 0.772 | | | |
| SMOS L2SMP_E Average V3 | 0.053 | | | -0.023 | | | 0.067 | | | 0.683 | | | | | |
| SMAP L2SMP_E Average V2 | 0.046 | 0.038 | 0.049 | -0.029 | -0.001 | 0.039 | 0.062 | 0.047 | 0.072 | 0.780 | 0.814 | 0.728 | | | |
| SMOS L2SMP_E Average V2 | 0.053 | | | -0.022 | | | 0.067 | | | 0.665 | | | | | |

Table 8.8. SMAP L2SMP_E Version 3 CVS Assessment for Ascending (PM) Overpasses

| CVS | ubRMSE (m ³ /m ³) | | | Bias (m ³ /m ³) | | | RMSE (m ³ /m ³) | | | R | | | N | | |
|--------------------------------|--|--------------|--------------|--|---------------|---------------|--|--------------|--------------|--------------|--------------|--------------|-------|-------|------|
| | SCA-H | SCA-V | MDCA | SCA-H | SCA-V | MDCA | SCA-H | SCA-V | MDCA | SCA-H | SCA-V | MDCA | SCA-H | SCA-V | MDCA |
| Reynolds Creek | 0.045 | 0.043 | 0.045 | -0.064 | -0.015 | -0.001 | 0.078 | 0.045 | 0.045 | 0.555 | 0.623 | 0.623 | 186 | 199 | 199 |
| Walnut Gulch | 0.026 | 0.024 | 0.028 | -0.030 | 0.003 | 0.009 | 0.039 | 0.024 | 0.029 | 0.696 | 0.751 | 0.745 | 384 | 507 | 510 |
| TxSON | 0.020 | 0.020 | 0.028 | -0.059 | -0.006 | 0.010 | 0.062 | 0.021 | 0.030 | 0.933 | 0.935 | 0.860 | 610 | 610 | 610 |
| Fort Cobb | 0.038 | 0.030 | 0.030 | -0.079 | -0.049 | -0.049 | 0.088 | 0.057 | 0.058 | 0.859 | 0.873 | 0.837 | 575 | 576 | 576 |
| Little Washita | 0.025 | 0.022 | 0.029 | -0.049 | -0.012 | -0.006 | 0.055 | 0.025 | 0.030 | 0.902 | 0.912 | 0.817 | 524 | 524 | 523 |
| South Fork | 0.063 | 0.046 | 0.056 | -0.048 | -0.044 | -0.063 | 0.079 | 0.063 | 0.085 | 0.715 | 0.770 | 0.645 | 358 | 361 | 361 |
| Little River | 0.043 | 0.036 | 0.041 | 0.020 | 0.061 | 0.048 | 0.047 | 0.071 | 0.063 | 0.782 | 0.764 | 0.635 | 443 | 444 | 443 |
| Kenaston | 0.037 | 0.025 | 0.040 | -0.023 | 0.007 | 0.016 | 0.044 | 0.026 | 0.043 | 0.819 | 0.884 | 0.727 | 352 | 352 | 352 |
| Carman | 0.081 | 0.052 | 0.050 | -0.056 | -0.053 | -0.068 | 0.099 | 0.074 | 0.084 | 0.550 | 0.656 | 0.594 | 281 | 283 | 283 |
| Monte Buey | 0.066 | 0.043 | 0.037 | -0.008 | -0.006 | -0.048 | 0.066 | 0.043 | 0.061 | 0.858 | 0.917 | 0.775 | 201 | 219 | 229 |
| REMEDHUS | 0.043 | 0.041 | 0.041 | -0.021 | 0.007 | 0.007 | 0.048 | 0.041 | 0.041 | 0.839 | 0.834 | 0.81 | 551 | 563 | 565 |
| Twente | 0.073 | 0.052 | 0.043 | 0.043 | 0.050 | -0.008 | 0.085 | 0.072 | 0.044 | 0.894 | 0.910 | 0.876 | 417 | 436 | 441 |
| HOBE | 0.047 | 0.034 | 0.050 | 0.015 | 0.006 | -0.041 | 0.050 | 0.035 | 0.065 | 0.687 | 0.849 | 0.783 | 117 | 117 | 117 |
| MAHASRI | 0.031 | 0.031 | 0.032 | -0.010 | 0.000 | 0.000 | 0.033 | 0.031 | 0.032 | 0.760 | 0.757 | 0.747 | 427 | 423 | 452 |
| Yanco | 0.051 | 0.041 | 0.037 | -0.009 | 0.016 | 0.004 | 0.052 | 0.044 | 0.037 | 0.928 | 0.936 | 0.924 | 438 | 442 | 447 |
| Mean Absolute Bias | | | | 0.035 | 0.022 | 0.025 | | | | | | | | | |
| SMAP L2SMP_E Average V3 | 0.046 | 0.036 | 0.039 | -0.025 | -0.002 | -0.013 | 0.062 | 0.045 | 0.050 | 0.785 | 0.825 | 0.760 | | | |
| SMOS L2SMP_E Average V3 | 0.052 | | | -0.029 | | | 0.068 | | | 0.701 | | | | | |
| SMAP L2SMP_E Average V2 | 0.045 | 0.036 | 0.047 | -0.024 | -0.002 | 0.031 | 0.061 | 0.045 | 0.066 | 0.780 | 0.818 | 0.712 | | | |
| SMOS L2SMP_E Average V2 | 0.055 | | | -0.026 | | | 0.068 | | | 0.677 | | | | | |

Table 8.9. SMAP L2SMP_E Version 3 Sparse Network Assessment for Descending (AM) Overpasses

| IGBP Class | ubRMSD (m ³ /m ³) | | | | Bias (m ³ /m ³) | | | | RMSD (m ³ /m ³) | | | | R | | | | N |
|--------------------------------|--|--------------|--------------|--------------|--|--------------|--------------|---------------|--|--------------|--------------|--------------|--------------|--------------|--------------|--------------|-----|
| | SCA-H | SCA-V | MDCA | SMOS | SCA-H | SCA-V | MDCA | SMOS | SCA-H | SCA-V | MDCA | SMOS | SCA-H | SCA-V | MDCA | SMOS | |
| Evergreen needleleaf forest | 0.035 | 0.034 | 0.036 | 0.094 | -0.024 | 0.031 | 0.057 | -0.042 | 0.050 | 0.049 | 0.067 | 0.123 | 0.732 | 0.736 | 0.693 | 0.017 | 2 |
| Evergreen broadleaf forest | | | | | | | | | | | | | | | | | |
| Deciduous needleleaf forest | | | | | | | | | | | | | | | | | |
| Deciduous broadleaf forest | | | | | | | | | | | | | | | | | |
| Mixed forest | 0.056 | 0.057 | 0.060 | 0.057 | -0.057 | -0.019 | -0.020 | -0.072 | 0.080 | 0.060 | 0.063 | 0.092 | 0.693 | 0.680 | 0.647 | 0.712 | 1 |
| Closed shrublands | | | | | | | | | | | | | | | | | |
| Open shrublands | 0.041 | 0.041 | 0.046 | 0.053 | -0.042 | 0.000 | 0.018 | -0.008 | 0.066 | 0.055 | 0.061 | 0.063 | 0.580 | 0.593 | 0.583 | 0.508 | 43 |
| Woody savannas | 0.060 | 0.056 | 0.060 | 0.095 | -0.019 | 0.028 | 0.023 | -0.053 | 0.090 | 0.088 | 0.088 | 0.140 | 0.713 | 0.732 | 0.657 | 0.435 | 19 |
| Savannas | 0.033 | 0.031 | 0.031 | 0.045 | -0.038 | -0.006 | -0.014 | -0.022 | 0.063 | 0.052 | 0.052 | 0.060 | 0.874 | 0.876 | 0.870 | 0.850 | 3 |
| Grasslands | 0.051 | 0.050 | 0.054 | 0.062 | -0.070 | -0.027 | -0.011 | -0.044 | 0.093 | 0.072 | 0.072 | 0.088 | 0.687 | 0.696 | 0.666 | 0.614 | 238 |
| Permanent wetlands | | | | | | | | | | | | | | | | | |
| Croplands | 0.077 | 0.066 | 0.066 | 0.080 | -0.038 | -0.011 | -0.011 | -0.046 | 0.113 | 0.098 | 0.098 | 0.116 | 0.559 | 0.601 | 0.555 | 0.545 | 61 |
| Urban and built-up | | | | | | | | | | | | | | | | | |
| Crop/Natural vegetation mosaic | 0.073 | 0.063 | 0.065 | 0.100 | -0.025 | 0.017 | 0.007 | -0.066 | 0.101 | 0.090 | 0.091 | 0.151 | 0.579 | 0.644 | 0.636 | 0.412 | 23 |
| Snow and ice | | | | | | | | | | | | | | | | | |
| Barren/Sparse | 0.023 | 0.023 | 0.025 | 0.031 | -0.015 | 0.014 | 0.024 | -0.003 | 0.036 | 0.035 | 0.04 | 0.039 | 0.644 | 0.633 | 0.638 | 0.532 | 6 |
| Mean Absolute Bias | | | | | 0.065 | 0.056 | 0.059 | 0.081 | | | | | | | | | |
| SMAP L2SMP_E Average V3 | 0.050 | 0.047 | 0.049 | 0.069 | -0.036 | 0.003 | 0.008 | -0.040 | 0.077 | 0.066 | 0.070 | 0.097 | 0.673 | 0.688 | 0.660 | 0.514 | |
| SMAP L2SMP_E Average V2 | 0.048 | 0.045 | 0.056 | 0.068 | -0.034 | 0.003 | 0.057 | -0.043 | 0.075 | 0.065 | 0.094 | 0.099 | 0.660 | 0.668 | 0.588 | 0.511 | |

Average is based upon all sets of observations, not the average of the land cover category results.

Table 8.10. SMAP L2SMP_E Version 3 Sparse Network Assessment for Ascending (PM) Overpasses

| IGBP Class | ubRMSD (m ³ /m ³) | | | | Bias (m ³ /m ³) | | | | RMSD (m ³ /m ³) | | | | R | | | | N |
|--------------------------------|--|--------------|--------------|--------------|--|--------------|--------------|---------------|--|--------------|--------------|--------------|--------------|--------------|--------------|--------------|-----|
| | SCA-H | SCA-V | MDCA | SMOS | SCA-H | SCA-V | MDCA | SMOS | SCA-H | SCA-V | MDCA | SMOS | SCA-H | SCA-V | MDCA | SMOS | |
| Evergreen needleleaf forest | 0.037 | 0.036 | 0.042 | 0.078 | -0.027 | 0.034 | 0.066 | -0.040 | 0.052 | 0.055 | 0.078 | 0.123 | 0.665 | 0.655 | 0.594 | 0.040 | 2 |
| Evergreen broadleaf forest | | | | | | | | | | | | | | | | | |
| Deciduous needleleaf forest | | | | | | | | | | | | | | | | | |
| Deciduous broadleaf forest | | | | | | | | | | | | | | | | | |
| Mixed forest | 0.057 | 0.055 | 0.055 | 0.057 | -0.049 | -0.013 | -0.017 | -0.056 | 0.075 | 0.056 | 0.057 | 0.080 | 0.699 | 0.727 | 0.728 | 0.715 | 1 |
| Closed shrublands | | | | | | | | | | | | | | | | | |
| Open shrublands | 0.041 | 0.041 | 0.046 | 0.056 | -0.046 | -0.003 | 0.016 | -0.005 | 0.066 | 0.054 | 0.061 | 0.069 | 0.569 | 0.560 | 0.535 | 0.435 | 43 |
| Woody savannas | 0.060 | 0.055 | 0.061 | 0.095 | -0.004 | 0.037 | 0.023 | -0.043 | 0.089 | 0.091 | 0.088 | 0.125 | 0.703 | 0.712 | 0.606 | 0.489 | 19 |
| Savannas | 0.035 | 0.033 | 0.034 | 0.049 | -0.031 | -0.001 | -0.013 | -0.023 | 0.062 | 0.055 | 0.056 | 0.071 | 0.868 | 0.85 | 0.835 | 0.772 | 3 |
| Grasslands | 0.051 | 0.049 | 0.053 | 0.062 | -0.065 | -0.025 | -0.014 | -0.042 | 0.090 | 0.072 | 0.073 | 0.086 | 0.694 | 0.701 | 0.662 | 0.621 | 238 |
| Permanent wetlands | | | | | | | | | | | | | | | | | |
| Croplands | 0.076 | 0.064 | 0.064 | 0.078 | -0.024 | -0.006 | -0.016 | -0.044 | 0.112 | 0.097 | 0.097 | 0.113 | 0.562 | 0.605 | 0.547 | 0.543 | 61 |
| Urban and built-up | | | | | | | | | | | | | | | | | |
| Crop/Natural vegetation mosaic | 0.073 | 0.063 | 0.065 | 0.098 | -0.001 | 0.030 | 0.007 | -0.061 | 0.098 | 0.091 | 0.091 | 0.141 | 0.565 | 0.633 | 0.604 | 0.436 | 23 |
| Snow and ice | | | | | | | | | | | | | | | | | |
| Barren/Sparse | 0.024 | 0.025 | 0.027 | 0.039 | -0.018 | 0.014 | 0.025 | -0.003 | 0.038 | 0.036 | 0.041 | 0.047 | 0.557 | 0.514 | 0.496 | 0.405 | 6 |
| Mean Absolute Bias | | | | | 0.063 | 0.057 | 0.061 | 0.079 | | | | | | | | | |
| SMAP L2SMP_E Average V3 | 0.050 | 0.047 | 0.049 | 0.068 | -0.029 | 0.007 | 0.009 | -0.035 | 0.076 | 0.067 | 0.071 | 0.095 | 0.654 | 0.662 | 0.623 | 0.495 | |
| SMAP L2SMP_E Average V2 | 0.049 | 0.046 | 0.056 | 0.067 | -0.028 | 0.008 | 0.059 | -0.039 | 0.074 | 0.067 | 0.096 | 0.097 | 0.633 | 0.635 | 0.540 | 0.497 | |

Average is based upon all sets of observations, not the average of the land cover category results.

8.3 Summary

Three alternative L2SMP retrieval algorithms were evaluated using three methodologies in preparation for this release. The algorithms included the Single Channel Algorithm–H Polarization (SCA-H), Single Channel Algorithm–V Polarization (SCA-V), and Modified Dual Channel Algorithm (MDCA). Assessment methodologies were Core Validation Sites (CVS), sparse networks, and intercomparisons with SMOS. **The baseline algorithm (SCA-V) remains unchanged for both L2 and L3 products.**

For the current validated release (Version 6) of L2SMP, the goal was to update the previous assessment of the retrieval algorithms on a larger period of time and to assess the new MDCA algorithm in comparison with DCA and with SCA-V. This assessment was supported by global analyses using sparse networks and SMOS intercomparisons as well as CVS matchups. These analyses indicated that the SCA-V had better unbiased root mean square error and correlation and lower bias than the SCA-H or MDCA. Based on these results, it is recommended that the SCA-V be continued as the operational baseline algorithm for this release. The overall ubRMSE of the SCA-V retrieved soil moisture from the descending (AM) orbits is $0.037 \text{ m}^3/\text{m}^3$, which is better than the project target accuracy ($0.040 \text{ m}^3/\text{m}^3$ ubRMSE or better). Overall bias has also been reduced significantly compared to earlier versions of the products.

Sparse network comparisons are more difficult to interpret due to upscaling but provide many more locations than the CVS. The analyses conducted here supported the conclusion reached in the CVS assessment, and contributed to improving validation through Triple Colocation analyses of uncertainties. The sparse network data also allowed the evaluation of performance based on land cover.

SMAP CVS and sparse network retrievals were compared to SMOS. These analyses supported the conclusions of prior assessments that the L2SMP currently has better performance metrics than SMOS.

The analyses described above were repeated for the L2SMP PM products. These show comparable performance to the AM results for all metrics. The comparable performance for AM and PM retrievals is attributed to the improved land surface temperature correction approach implemented in the previous version and continued in this release.

The L2SMP_E Version 3 product was assessed using CVS chosen specifically to exploit the L2SMP_E grid posting (9 km) and contributing domain (33 km). Results were essentially the same as those obtained in the L2SMP Version 6 analyses.

Based on the extensive validation analyses to date, the number of peer-reviewed publications (including the numerous independent investigations noted in the bibliography section), the length of the SMAP period of record, and the utilization of feedback of validation in a systematic update, with this version of L2SMP and L2SMP_E the team has completed CEOS Stage 4 validation [10]. The Cal/Val program will continue throughout the mission with the goals of increasing the robustness of the soil moisture products and addressing specific site issues.

9 OUTLOOK AND FUTURE PLANS

Satellite passive microwave retrieval of soil moisture has been the subject of intensive study and assessment for the past several decades. Over this time there have been improvements in the microwave instruments used, primarily in the availability of L-band sensors on orbit. However, sensor resolution has remained roughly the same over this period, which is actually an achievement considering the increase in sensor wavelength from X band to C band to L band over the years. With spatial resolution in the 25-50 km range, there will always be heterogeneity within the satellite footprint that will influence the accuracy of the retrieved soil moisture as well as its validation. Precipitation types and patterns are one of the biggest contributors to this heterogeneity. As a result, one should not expect that the validation metric ubRMSE will ever approach zero except in very homogeneous domains. In contrast, bias tends to be indicative of a systematic error, possibly related to algorithm parameterization and model structure. High quality data are needed to discover and address these systematic errors. Some issues that should be considered during the extended SMAP mission include:

- *Increasing the number of CVS.* There are several candidate calibration/validation sites that may yet qualify as CVS. Several will require additional time for further development (such as Millbrook, Kuwait, India).
- *Evaluate the impacts of algorithm structure and components on retrieval.* There are some aspects of soil moisture retrieval algorithms that are used because they facilitate operational soil moisture retrieval. One of these simplifying aspects is the use of the Fresnel equations that specify that conditions in the microwave contributing depth are uniform. While there is ample evidence that this is true in most cases, it should be recognized that this assumption is a potential source of error – some effort should be made to evaluate when and where it limits soil moisture retrieval accuracy. Another assumption is that a single dielectric mixing model applies under all conditions globally. All of the commonly-used dielectric models are highly dependent on the robustness of the data set used in their development. The impact of this assumption on retrieval error needs further evaluation. Another consideration in the current MDCA is the assumption of equality of the vegetation parameters for the H and V polarizations. This assumption does simplify retrieval but it is not valid for all categories of vegetation.
- *Optimization of algorithm parameters.* The current release retains the same set of algorithm parameters used previously in SMAP Data Versions 2 to 5 for the single channel algorithms. However, the MDCA utilizes a separate set of albedo and roughness parameters specific to that algorithm. Because the current algorithm parameters do not vary in time, they are likely to be inadequate for producing accurate retrieval results in agricultural areas where there is often high temporal variability of vegetation amount, land cover heterogeneity, and terrain roughness due to tillage. Initial attempts with spatio-temporal optimization of algorithm parameters have resulted in modest gains in retrieval performance at CVS. Full implementation of the optimization results would require more rigorous validation involving sparse network comparison in addition to CVS comparison, as well as a significant redesign of the current SMAP operational processing codes. It is anticipated that the benefits of using more optimal coefficients will be demonstrated in future releases of the L2SMP product, along with other improvements.
- *Possible subdivision of crop land cover class into distinct crop subclasses.* Another source of error is SMAP's use of a single IGBP land cover class to cover the great variety of global crops. One area of future work will examine the possibility of subdividing the single crop class into a number of distinct subclasses (e.g., corn, soybeans, wheat, rice) with appropriate parameterization which would better represent the main global crop structural categories. Due to the latency problem in

acquiring up-to-date crop maps, this issue is not likely to be addressed until the final bulk reprocessing of SMAP data.

- *Incorporating field campaign results into algorithm assessments and improvements.* Several SMAP field campaigns were conducted postlaunch. Analyses of the data are ongoing and results from these field campaigns will be used in future assessments and algorithm improvements. It is expected that the results of the Iowa and Manitoba campaigns in 2016 will be of great value in resolving the significant error in soil moisture retrievals at these CVS (South Fork and Carmen).
- *Precipitation flag improvement.* Satellite observations made shortly after (or during) a rain event can be difficult to interpret and use in validation. A wet surface will dominate what the radiometer observes, which may be much wetter than at the 5 cm depth of an *in situ* sensor (due to the lag time for the wetting front to infiltrate down to the *in situ* sensor depth). Smaller precipitation events may be more problematic than larger events that wet a thicker surface layer. The divergence in these satellite observations will also be dependent on antecedent conditions (i.e., rain on a very dry soil). At the present time the GMAO model precipitation forecast for the three hours preceding a SMAP overpass at a given site is used. There is evidence that this approach is not adequate and that a longer time window might be necessary. However, achieving a longer time window for the SMAP precipitation flag will require additional/alternative processing of the GMAO data. Additionally, a comparison between using GMAO forecast model data and the GPM blended satellite data for the SMAP precipitation flag has begun.
- *Improvement of retrievals over forests.* Dense forests (where $VWC > 5 \text{ kg/m}^2$) typically exceed the currently accepted threshold for accurate soil moisture retrieval. SMAP provides a flagged retrieval over forests, and the spatial extent of these flagged areas is quite large. At this point there is no supporting validation of the L2SMP soil moisture retrieved for forest areas, and the SMAP forest retrievals are quite different from SMOS. While extending accurate soil moisture retrievals to forests would likely be very beneficial to a variety of end users of the data, the SMAP team has little confidence in the accuracy and the appropriateness of the current baseline retrieval approach for soil moisture retrieval in forests. The SMAPVEX20 field campaign will collect data in two temperate forests (Millbrook, NY and Harvard Forest, MA) to begin to address soil moisture retrieval in forested areas. Future efforts to improve these retrievals should include both a careful evaluation of alternative algorithms and improving validation resources through a combination of CVS, temporary networks, and additional field campaigns.

10 ACKNOWLEDGEMENTS

This document resulted from many hours of diligent analyses and constructive discussion among the L2SMP Team, Cal/Val Partners, and other members of the SMAP Project Team.

11 REFERENCES

- [1] Jackson, T., P. O'Neill, S. Chan, R. Bindlish, A. Colliander, F. Chen, M. Burgin, S. Dunbar, J. Piepmeier, M. Cosh, T. Caldwell, J. Walker, X. Wu, A. Berg, T. Rowlandson, A. Pacheco, H. McNairn, M. Thibeault, J. Martínez-Fernández, Á. González-Zamora, E. Lopez-Baeza, F. Udall, M. Seyfried, D. Bosch, P. Starks, C. Holifield, J. Prueger, Z. Su, R. van der Velde, J. Asanuma, M. Palecki, E. Small, M. Zreda, J. Calvet, W. Crow, Y. Kerr, S. Yueh, and D. Entekhabi, June 6, 2018. Calibration and Validation for the L2/3_SM_P Version 5 and L2/3_SM_P_E Version 2 Data Products, SMAP Project, JPL D-56297, Jet Propulsion Laboratory, Pasadena, CA.
- [2] Chan, S., Bindlish, R., O'Neill, P., Njoku, E., Jackson, T. J., Colliander, A., Chen, F., Burgin, M., Dunbar, R.S., Piepmeier, J., Yueh, S., Entekhabi, D., Cosh, M.H., Caldwell, T., Walker, J., Wu, X., Berg, A., Rowlandson, T., Pacheco, A., McNairn, H., Thibeault, M., Martinez-Fernandez, J., Gonzalez-Zamora, A., Seyfried, M., Bosch, D., Starks, P., Goodrich, D., Prueger, J., Palecki, M., Small, E.E., Zreda, M., Calvet, J.-C., Crow, W.T., and Kerr, Y. Assessment of the SMAP level 2 passive soil moisture product. *IEEE Transactions on Geoscience and Remote Sensing*, 54 (8): 4994-5007, 2016, doi: 10.1109/TGRS.2016.2561938.
- [3] Chan, S., Bindlish, R., O'Neill, P.E., Jackson, T.J., Njoku, E., Dunbar, R.S., Chaubell, J., Peipmeier, J., Yueh, S., Entekhabi, D., Colliander, A., Chen, F., Cosh, M.H., Caldwell, T., Walker, J., Berg, A., McNairn, H., Thibeault, M., Martinez-Fernandez, J., Udall, F., Seyfried, M.S., Bosch, D.D., Starks, P., Holyfield Collins, C., and Prueger, J.H. Development and assessment of the SMAP enhanced passive soil moisture product. *Remote Sensing of Environment*, 204: 931-941. 2018.
- [4] Colliander, A., Jackson, T.J., Chan, S., O'Neill, P.E., Bindlish, R., Cosh, M.H., Berg, A., Rowlandson, T., Bosch, D., Caldwell, Walker, J.P., Berg, A., McNairn, H., Thibeault, M., Martínez-Fernández, J., Jensen, K.H., Asanuma, J., Seyfried, M., Bosch, D.D., Starks, P., Holifield Collins, C., Prueger, J.H., Su, Z., Lopez-Baeza, E., and Yueh, S.H. An assessment of the differences between spatial resolution and grid size for the SMAP enhanced soil moisture product over homogeneous sites. *Remote Sensing of Environment*, 207: 65-70. 2018.
- [5] Chen, F., Crow, W. T., Colliander, A., Cosh, M., Jackson, T. J., Bindlish, R., Reichle, R., Chan, S. K., Bosch, D. D., Starks, P. S., Goodrich, D. C., and Seyfried, M. S. Application of triple collocation in ground-based validation of Soil Moisture Active Passive (SMAP) Level 2 data products. *IEEE Journal of Selected Topics in Applied Earth Observations and Remote Sensing*, 10: 489-502. 2017.
- [6] Jackson, T. J., Colliander, A., Kimball, J., Reichle, R., Crow, W., Entekhabi, D. et al. Science data calibration and validation plan, Release A, JPL D-52544, March 14, 2014.
- [7] O'Neill, P., Bindlish, R, Chan, S., Njoku, E., Chaubell, J., and Jackson, T. SMAP algorithm theoretical basis document (ATBD): L2/3_SM_P, Revision E, JPL D-66480, Jet Propulsion Laboratory, Pasadena, CA, August 15, 2019.
- [8] Entekhabi, D., Yueh, S., O'Neill, P., Kellogg, K. et al., SMAP Handbook, JPL Publication JPL 400-1567, Jet Propulsion Laboratory, Pasadena, California, 182 pages, July, 2014.
- [9] SMAP Level 1 Mission Requirements and Success Criteria. (Appendix O to the Earth Systematic Missions Program Plan: Program-Level Requirements on the Soil Moisture Active Passive Project.), NASA Headquarters/Earth Science Division, Washington, DC, version 5, 2013.
- [10] Committee on Earth Observation Satellites (CEOS) Working Group on Calibration and Validation (WGCV): <http://calvalportal.ceos.org/CalValPortal/welcome.do> and WWW: Land Products Sub-Group of Committee on Earth Observation Satellites (CEOS) Working Group on Calibration and Validation (WGCV): <http://lpvs.gsfc.nasa.gov>.

- [11] Peng, J., Misra, S., Piepmeier, J.R., Dinnat, E.P., Hudson, D., Le Vine, D.M., De Amici, G., Mohammed, P.N., Bindlish, R., Yueh, S.H., Meissner, T., and Jackson, T. J. Soil moisture active/passive (SMAP) L-band microwave radiometer post-launch calibration. *IEEE Trans. Geoscience and Remote Sensing*, 55(4): 1897-1914. 2017.
- [12] SMAP Algorithm Theoretical Basis Document: Enhanced L1B_TB_E Radiometer Brightness Temperature Data Product. SMAP Project, JPL D-56287, Jet Propulsion Laboratory, Pasadena, CA.
- [13] Piepmeier, J., P. Mohammed, G. De Amici, E. Kim, J. Peng, C. Ruf, and M. Chaubell. SMAP Algorithm Theoretical Basis Document: L1B Radiometer Product. Revision C, June 6, 2018, SMAP Project, GSFC-SMAP-006, NASA Goddard Space Flight Center, Greenbelt, MD.
- [14] Dawson, D., SMAP radiometer error budget, SMAP Project, JPL D-61632, Jet Propulsion Laboratory, Pasadena, CA.
- [15] Mironov, V. L., Kosolapova, L. G., and Fomin, S. V. Physically and mineralogically based spectroscopic dielectric model for moist soils. *IEEE Trans. Geosci. Remote Sens.*, 47(7): 2059-2070. 2009.
- [16] Choudhury, B.J. and Schmugge, T.J. A parameterization of effective soil temperature for microwave emission. *Journal of Geophysical Research*, 87(C2): 1301-1304.1982.
- [17] Dorigo, W. A., Xaver, A., Vreugdenhil, M., Gruber, A., Hegyiova, A, Sanchis-Dufau, A. D., Zamojski, D., Cordes, C., Wagner, W., and Drusch, M. Global automated quality control of in situ soil moisture data from the international soil moisture network. *Vadose Zone Journal*, 12. doi:10.2136/vzj2012.0097. 2012.
- [18] Adams, J. R., McNairn, H., Berg, A. A., and Champagne, C. Evaluation of near-surface soil moisture data from an AAFC monitoring network in Manitoba, Canada: Implications for L-band satellite validation. *Journal of Hydrology*, 521: 82-592. 2015.
- [19] Lawrence, H., Wigneron, J. -P., Demontoux, F., Mialon, A., and Kerr, Y. H. (2013). “Evaluating the Semiempirical H-Q Model Used to Calculate the L-Band Emissivity of a Rough Bare Soil”, *IEEE Transactions on Geoscience and Remote Sensing*, 51(7), 4075–4084.

12 BIBLIOGRAPHY OF PUBLISHED SMAP L2SMP and L2SMP_E VALIDATION STUDIES

Please see the following link for more SMAP-related papers: <https://nsidc.org/data/smap/research.html>

Chen, F., Crow, W.T., Bindlish, R., Colliander, A., Burgin, M.S., Asanuma, J., Aida, K. “Global-scale evaluation of SMAP, SMOS and ASCAT soil moisture products using triple collocation,” (2018) *Remote Sensing of Environment*, 214, pp. 1-13. DOI: 10.1016/j.rse.2018.05.008

Santi, E., Paloscia, S., Pettinato, S., Brocca, L., Ciabatta, L., Entekhabi, D. “Integration of microwave data from SMAP and AMSR2 for soil moisture monitoring in Italy.” (2018) *Remote Sensing of Environment*, 212, pp. 21-30. DOI: 10.1016/j.rse.2018.04.039

Zhao, Y., Mouche, A.A., Chapron, B., Reul, N. “Direct Comparison Between Active C-Band Radar and Passive L-Band Radiometer Measurements: Extreme Event Cases,” (2018) *IEEE Geoscience and Remote Sensing Letters*, in press. DOI: 10.1109/LGRS.2018.2811712

Li, C., Lu, H., Yang, K., Han, M., Wright, J.S., Chen, Y., Yu, L., Xu, S., Huang, X., Gong, W. “The evaluation of SMAP enhanced soil moisture products using high-resolution model simulations and in-situ observations on the Tibetan Plateau,” (2018) *Remote Sensing*, 10(4), art. #535. DOI: 10.3390/rs10040535

El Hajj, M., Baghdadi, N., Zribi, M., Rodríguez-Fernández, N., Wigneron, J.P., Al-Yaari, A., Al Bitar, A., Albergel, C., Calvet, J.-C. “Evaluation of SMOS, SMAP, ASCAT and Sentinel-1 soil moisture products at sites in Southwestern France,” (2018) *Remote Sensing*, 10 (4), art. #569. DOI: 10.3390/rs10040569

Zheng, D., van der Velde, R., Wen, J., Wang, X., Ferrazzoli, P., Schwank, M., Colliander, A., Bindlish, R., Su, Z. “Assessment of the SMAP Soil Emission Model and Soil Moisture Retrieval Algorithms for a Tibetan Desert Ecosystem,” (2018) *IEEE Transactions on Geoscience and Remote Sensing*, in press. DOI: 10.1109/TGRS.2018.2811318

Colliander, A., Jackson, T.J., Chan, S.K., O'Neill, P., Bindlish, R., Cosh, M.H., Caldwell, T., Walker, J.P., Berg, A., McNairn, H., Thibeault, M., Martínez-Fernández, J., Jensen, K.H., Asanuma, J., Seyfried, M.S., Bosch, D.D., Starks, P.J., Holifield Collins, C., Prueger, J.H., Su, Z., Lopez-Baeza, E., Yueh, S.H. “An assessment of the differences between spatial resolution and grid size for the SMAP enhanced soil moisture product over homogeneous sites,” (2018) *Remote Sensing of Environment*, 207, pp. 65-70. DOI: 10.1016/j.rse.2018.02.006

Xiong, L., Yang, H., Zeng, L., Xu, C.-Y. “Evaluating consistency between the remotely sensed soil moisture and the hydrological model-simulated soil moisture in the Qujiang catchment of China,” (2018) *Water (Switzerland)*, 10 (3), art. #291. DOI: 10.3390/w10030291

Chen, Q., Zeng, J., Cui, C., Li, Z., Chen, K.-S., Bai, X., Xu, J. “Soil Moisture Retrieval from SMAP: A Validation and Error Analysis Study Using Ground-Based Observations over the Little Washita Watershed,” (2018) *IEEE Transactions on Geoscience and Remote Sensing*, 56 (3), pp. 1398-1408. DOI: 10.1109/TGRS.2017.2762462

Gao, Y., Walker, J., Ye, N., Panciera, R., Monerris, A., Ryu, D., Rudiger, C., Jackson, T. "Evaluation of the Tau-Omega Model for Passive Microwave Soil Moisture Retrieval Using SMAPEX Datasets," (2018) IEEE Journal of Selected Topics in Applied Earth Observations and Remote Sensing, 11 (3), pp. 888-895. DOI: 10.1109/JSTARS.2018.2796546

Dong, J., Crow, W.T., Bindlish, R. "The Error Structure of the SMAP Single and Dual Channel Soil Moisture Retrievals," (2018) Geophysical Research Letters, 45 (2), pp. 758-765. DOI: 10.1002/2017GL075656

Santi, E., Paloscia, S., Pettinato, S., Brocca, L., Ciabatta, L., Entekhabi, D. "On the synergy of SMAP, AMSR2 AND SENTINEL-1 for retrieving soil moisture," (2018) International Journal of Applied Earth Observation and Geoinformation, 65, pp. 114-123. DOI: 10.1016/j.jag.2017.10.010

Chew, C.C., Small, E.E. "Soil Moisture Sensing Using Spaceborne GNSS Reflections: Comparison of CYGNSS Reflectivity to SMAP Soil Moisture," (2018) Geophysical Research Letters, in press. DOI: 10.1029/2018GL077905

Kim, H., Parinussa, R., Konings, A.G., Wagner, W., Cosh, M.H., Lakshmi, V., Zohaib, M., Choi, M. "Global-scale assessment and combination of SMAP with ASCAT (active) and AMSR2 (passive) soil moisture products," (2018) Remote Sensing of Environment, 204, pp. 260-275. DOI: 10.1016/j.rse.2017.10.026

Chan, S.K., Bindlish, R., O'Neill, P., Jackson, T., Njoku, E., Dunbar, S., Chaubell, J., Piepmeier, J., Yueh, S., Entekhabi, D., Colliander, A., Chen, F., Cosh, M.H., Caldwell, T., Walker, J., Berg, A., McNairn, H., Thibeault, M., Martinez-Fernandez, J., Uldall, F., Seyfried, M., Bosch, D., Starks, P., Holifield Collins, C., Prueger, J., van der Velde, R., Asanuma, J., Palecki, M., Small, E.E., Zreda, M., Calvet, J., Crow, W.T., Kerr, Y. "Development and assessment of the SMAP enhanced passive soil moisture product," (2018) Remote Sensing of Environment, 204, pp. 931-941. DOI: 10.1016/j.rse.2017.08.025

Kolassa, J., Reichle, R.H., Liu, Q., Alemohammad, S.H., Gentine, P., Aida, K., Asanuma, J., Bircher, S., Caldwell, T., Colliander, A., Cosh, M., Holifield Collins, C., Jackson, T.J., Martinez-Fernandez, J., McNairn, H., Pacheco, A., Thibeault, M., Walker, J. "Estimating surface soil moisture from SMAP observations using a Neural Network technique," (2018) Remote Sensing of Environment, 204, pp. 43-59. DOI: 10.1016/j.rse.2017.10.045

Cui, C., Xu, J., Zeng, J., Chen, K.-S., Bai, X., Lu, H., Chen, Q., Zhao, T. "Soil moisture mapping from satellites: An intercomparison of SMAP, SMOS, FY3B, AMSR2, and ESA CCI over two dense network regions at different spatial scales," (2018) Remote Sensing, 10 (1), art. #33. DOI: 10.3390/rs10010033

Kumar, S.V., Dirmeyer, P.A., Peters-Lidard, C.D., Bindlish, R., Bolten, J. "Information theoretic evaluation of satellite soil moisture retrievals," (2018) Remote Sensing of Environment, 204, pp. 392-400. DOI: 10.1016/j.rse.2017.10.016

Colliander, A., Jackson, T.J., Cosh, M., Misra, S., Bindlish, R., Powers, J., McNairn, H., Bullock, P., Berg, A., Magagi, R., O'Neill, P., Yueh, S. "Soil moisture retrieval with airborne PALS instrument over agricultural areas in SMAPVEX16," (2017) International Geoscience and Remote Sensing Symposium (IGARSS), 2017-July, art. #8127864, pp. 3949-3952. DOI: 10.1109/IGARSS.2017.8127864

O'Neill, P., Chan, S., Bindlish, R., Jackson, T., Colliander, A., Dunbar, S., Chen, F., Piepmeier, J., Yueh, S., Entekhabi, D., Cosh, M., Caldwell, T., Walker, J., Wu, X., Berg, A., Rowlandson, T., Pacheco, A., McNairn, H., Thibeault, M., Martinez-Fernandez, J., Gonzalez-Zamora, A., Lopez-Baeza, E., Udall, F.,

Seyfried, M., Bosch, D., Starks, P., Holifield, C., Prueger, J., Su, Z., Van Der Velde, R., Asanuma, J., Palecki, M., Small, E., Zreda, M., Calvet, J.-C., Crow, W., Kerr, Y. "Assessment of version 4 of the SMAP passive soil moisture standard product," (2017) Intl. Geoscience and Remote Sensing Symposium (IGARSS), 2017-July, art. no. 8127862, pp. 3941-3944. DOI: 10.1109/IGARSS.2017.8127862

Fascetti, F., Pierdicca, N., Pulvirenti, L., Crapolicchio, R. "Error characterization of SMOS, ASCAT, SMAP, ERA and ISMN soil moisture products: Automatic detection of cross-correlation error through extended quadruple collocation," (2017) International Geoscience and Remote Sensing Symposium (IGARSS), 2017-July, art. #8127916, pp. 4154-4157. DOI: 10.1109/IGARSS.2017.8127916

Chan, S., Bindlish, R., O'Neill, P., Jackson, T., Chaubell, J., Piepmeier, J., Dunbar, S., Colliander, A., Chen, F., Entekhabi, D., Yueh, S., Cosh, M., Caldwell, T., Walker, J., Wu, X., Berg, A., Rowlandson, T., Pacheco, A., McNairn, H., Thibeault, M., Martinez-Fernandez, J., Gonzalez-Zamora, A., Lopez-Baeza, E., Uldall, F., Seyfried, M., Bosch, D., Starks, P., Collins, C.H., Prueger, J., Su, Z., Van Der Velde, R., Asanuma, J., Palecki, M., Small, E., Zreda, M., Calvet, J.-C., Crow, W., Kerr, Y. "Development and validation of the SMAP enhanced passive soil moisture product," (2017) Intl. Geoscience and Remote Sensing Symposium (IGARSS), art. #8127512, pp. 2539-2542. DOI: 10.1109/IGARSS.2017.8127512

Cui, H., Jiang, L., Lu, Z., Wang, G., Wang, J. "Improvement and validation of QP model with dual-channel soil moisture retrieval algorithm in Genhe, China," (2017) International Geoscience and Remote Sensing Symposium (IGARSS), art. #8128115, pp. 4951-4954. DOI: 10.1109/IGARSS.2017.8128115

Cosh, M.H., Jackson, T.J., Starks, P., Bosch, D., Collins, C.H., Seyfried, M., Prueger, J., Livingston, S., Bindlish, R. "Strategies for validating satellite soil moisture products using in situ networks: Lessons from the USDA-ARS watersheds," (2017) International Geoscience and Remote Sensing Symposium (IGARSS), July 2017, art. #8127377, pp. 2015-2018. DOI: 10.1109/IGARSS.2017.8127377

Zhang, L., He, C., Zhang, M. "Multi-scale evaluation of the SMAP product using sparse in-situ network over a high mountainous Watershed, Northwest China," (2017) Remote Sensing, 9 (11), art. #1111. DOI: 10.3390/rs9111111

Karthikeyan, L., Pan, M., Wanders, N., Kumar, D.N., Wood, E.F. "Four decades of microwave satellite soil moisture observations: Part 2. Product validation and inter-satellite comparisons," (2017) Advances in Water Resources, 109, pp. 236-252. DOI: 10.1016/j.advwatres.2017.09.010

Karthikeyan, L., Pan, M., Wanders, N., Kumar, D.N., Wood, E.F. "Four decades of microwave satellite soil moisture observations: Part 1. A review of retrieval algorithms," (2017) Advances in Water Resources, 109, pp. 106-120. DOI: 10.1016/j.advwatres.2017.09.006

Liu, D., Mishra, A.K., Yu, Z., Yang, C., Konapala, G., Vu, T. "Performance of SMAP, AMSR-E and LAI for weekly agricultural drought forecasting over continental U.S.," (2017) Journal of Hydrology, 553, pp. 88-104. DOI: 10.1016/j.jhydrol.2017.07.049

Pierdicca, N., Fascetti, F., Pulvirenti, L., Crapolicchio, R. "Error Characterization of Soil Moisture Satellite Products: Retrieving Error Cross-Correlation Through Extended Quadruple Collocation," (2017) IEEE Journal of Selected Topics in Applied Earth Observations and Remote Sensing, 10 (10), art. #7964667, pp. 4522-4530. DOI: 10.1109/JSTARS.2017.2714025

Cui, H., Jiang, L., Du, J., Zhao, S., Wang, G., Lu, Z., Wang, J. "Evaluation and analysis of AMSR-2, SMOS, and SMAP soil moisture products in the Genhe area of China," (2017) Journal of Geophysical Research: Atmospheres, 122 (16), pp. 8650-8666. DOI: 10.1002/2017JD026800

Lee, J.H., Zhao, C., Kerr, Y. “Stochastic bias correction and uncertainty estimation of satellite-retrieved soil moisture products,” (2017) *Remote Sensing*, 9 (8), pp. 1-23. DOI: 10.3390/rs9080847

Colliander, A., Cosh, M.H., Misra, S., Jackson, T.J., Crow, W.T., Chan, S., Bindlish, R., Chae, C., Holifield Collins, C., Yueh, S.H. “Validation and scaling of soil moisture in a semi-arid environment: SMAP validation experiment 2015 (SMAPVEX15),” (2017) *Remote Sensing of Environment*, 196, pp. 101-112. DOI: 10.1016/j.rse.2017.04.022

Clewley, D., Whitcomb, J.B., Akbar, R., Silva, A.R., Berg, A., Adams, J.R., Caldwell, T., Entekhabi, D., Moghaddam, M. “A method for upscaling in situ soil moisture measurements to satellite footprint scale using Random Forests,” (2017) *IEEE Journal of Selected Topics in Applied Earth Observations and Remote Sensing*, 10 (6), art. #7907192, pp. 2663-2673. DOI: 10.1109/JSTARS.2017.2690220

Ray, R.L., Fares, A., He, Y., Temimi, M. “Evaluation and inter-comparison of satellite soil moisture products using in situ observations over Texas, U.S.,” (2017) *Water (Switzerland)*, 9 (6), art. #372. DOI: 10.3390/w9060372

Wrona, E., Rowlandson, T.L., Nambiar, M., Berg, A.A., Colliander, A., Marsh, P. “Validation of the Soil Moisture Active Passive (SMAP) satellite soil moisture retrieval in an Arctic tundra environment,” (2017) *Geophysical Research Letters*, 44 (9), pp. 4152-4158. DOI: 10.1002/2017GL072946

Burgin, M.S., Colliander, A., Njoku, E.G., Chan, S.K., Cabot, F., Kerr, Y.H., Bindlish, R., Jackson, T.J., Entekhabi, D., Yueh, S.H. “A Comparative Study of the SMAP Passive Soil Moisture Product with Existing Satellite-Based Soil Moisture Products,” (2017) *IEEE Transactions on Geoscience and Remote Sensing*, 55 (5), art. #7855655, pp. 2959-2971. DOI: 10.1109/TGRS.2017.2656859

Al-Yaari, A., Wigneron, J.-P., Kerr, Y., Rodriguez-Fernandez, N., O'Neill, P.E., Jackson, T.J., De Lannoy, G.J.M., Al Bitar, A., Mialon, A., Richaume, P., Walker, J.P., Mahmoodi, A., Yueh, S. “Evaluating soil moisture retrievals from ESA's SMOS and NASA's SMAP brightness temperature datasets,” (2017) *Remote Sensing of Environment*, 193, pp. 257-273. DOI: 10.1016/j.rse.2017.03.010

Ma, C., Li, X., Wei, L., Wang, W. “Multi-scale validation of SMAP soil moisture products over cold and arid regions in Northwestern China using distributed ground observation data,” (2017) *Remote Sensing*, 9(4), art. #327. DOI: 10.3390/rs9040327

Cai, X., Pan, M., Chaney, N.W., Colliander, A., Misra, S., Cosh, M.H., Crow, W.T., Jackson, T.J., Wood, E.F. “Validation of SMAP soil moisture for the SMAPVEX15 field campaign using a hyper-resolution model,” (2017) *Water Resources Research*, 53 (4), pp. 3013-3028. DOI: 10.1002/2016WR019967

Wigneron, J.-P., Jackson, T.J., O'Neill, P., De Lannoy, G., de Rosnay, P., Walker, J.P., Ferrazzoli, P., Mironov, V., Bircher, S., Grant, J.P., Kurum, M., Schwank, M., Munoz-Sabater, J., Das, N., Royer, A., Al-Yaari, A., Al Bitar, A., Fernandez-Moran, R., Lawrence, H., Mialon, A., Parrens, M., Richaume, P., Delwart, S., Kerr, Y. “Modelling the passive microwave signature from land surfaces: A review of recent results and application to the L-band SMOS & SMAP soil moisture retrieval algorithms,” (2017) *Remote Sensing of Environment*, 192, pp. 238-262. DOI: 10.1016/j.rse.2017.01.024

Colliander, A., Jackson, T.J., Bindlish, R., Chan, S., Das, N., Kim, S.B., Cosh, M.H., Dunbar, R.S., Dang, L., Pashaian, L., Asanuma, J., Aida, K., Berg, A., Rowlandson, T., Bosch, D., Caldwell, T., Caylor, K., Goodrich, D., al Jassar, H., Lopez-Baeza, E., Martinez-Fernandez, J., Gonzalez-Zamora, A., Livingston, S., McNairn, H., Pacheco, A., Moghaddam, M., Montzka, C., Notarnicola, C., Niedrist, G., Pellarin, T.,

Prueger, J., Pulliainen, J., Rautiainen, K., Ramos, J., Seyfried, M., Starks, P., Su, Z., Zeng, Y., van der Velde, R., Thibeault, M., Dorigo, W., Vreugdenhil, M., Walker, J.P., Wu, X., Moneris, A., O'Neill, P.E., Entekhabi, D., Njoku, E.G., Yueh, S. "Validation of SMAP surface soil moisture products with core validation sites," (2017) *Rem. Sens. of Environment*, 191, pp. 215-231. DOI: 10.1016/j.rse.2017.01.021

Sun, Y., Huang, S., Ma, J., Li, J., Li, X., Wang, H., Chen, S., Zang, W. "Preliminary evaluation of the SMAP radiometer soil moisture product over China using *in situ* data," (2017) *Remote Sensing*, 9 (3), art. #292. DOI: 10.3390/rs9030292

Chen, F., Crow, W.T., Colliander, A., Cosh, M.H., Jackson, T.J., Bindlish, R., Reichle, R.H., Chan, S.K., Bosch, D.D., Starks, P.J., Goodrich, D.C., Seyfried, M.S. "Application of Triple Collocation in Ground-Based Validation of Soil Moisture Active/Passive (SMAP) Level 2 Data Products," (2017) *IEEE Journal of Selected Topics in Applied Earth Observations and Remote Sensing*, 10 (2), art. #7493654, pp. 489-502. DOI: 10.1109/JSTARS.2016.2569998

Zhang, X., Zhang, T., Zhou, P., Shao, Y., Gao, S. "Validation analysis of SMAP and AMSR2 soil moisture products over the United States using ground-based measurements," (2017) *Remote Sensing*, 9 (2), art. no. 104. DOI: 10.3390/rs9020104

Chen, Y., Yang, K., Qin, J., Cui, Q., Lu, H., La, Z., Han, M., Tang, W. "Evaluation of SMAP, SMOS, and AMSR2 soil moisture retrievals against observations from two networks on the Tibetan Plateau," (2017) *Journal of Geophysical Research*, 122 (11), pp. 5780-5792. DOI: 10.1002/2016JD026388

Ye, N., Walker, J., Wu, X., Jackson, T., Renzullo, L., Merlin, O., Rudiger, C., Entekhabi, D., Dejeu, R., Kim, E. "Towards validation of SMAP: SMAPEX-4 & SMAPEX-5," (2016) *Intl. Geoscience and Rem. Sens. Symposium (IGARSS)*, art. #7729897, pp. 3469-3472. DOI: 10.1109/IGARSS.2016.7729897

Santi, E., Paloscia, S., Pettinato, S., Entekhabi, D., Alemohammad, S.H., Konings, A.G. "Integration of passive and active microwave data from SMAP, AMSR2 and Sentinel-1 for soil moisture monitoring," (2016) *International Geoscience and Remote Sensing Symposium (IGARSS)*, 2016-November, art. #7730368, pp. 5252-5255. DOI: 10.1109/IGARSS.2016.7730368

Zeng, J., Chen, K.-S., Bi, H., Chen, Q., Yuan, L. "A preliminary assessment of the SMAP radiometer soil moisture product using three *in situ* networks," (2016) *Intl. Geoscience and Rem. Sens. Symposium (IGARSS)*, art. #7729418, pp. 1637-1640. DOI: 10.1109/IGARSS.2016.7729418

Bindlish, R., Jackson, T.J., Piepmeier, J.R., Yueh, S., Kerr, Y. "Intercomparison of SMAP, SMOS and Aquarius L-band brightness temperature observations," (2016) *Intl. Geoscience and Remote Sensing Symposium (IGARSS)*, art. #7729527, pp. 2043-2046. DOI: 10.1109/IGARSS.2016.7729527

O'Neill, P., Chan, S., Colliander, A., Dunbar, S., Njoku, E., Bindlish, R., Chen, F., Jackson, T., Burgin, M., Piepmeier, J., Yueh, S., Entekhabi, D., Cosh, M., Caldwell, T., Walker, J., Wu, X., Berg, A., Rowlandson, T., Pacheco, A., McNairn, H., Thibeault, M., Martinez-Fernandez, J., Gonzalez-Zamora, A., Seyfried, M., Bosch, D., Starks, P., Goodrich, D., Prueger, J., Palecki, M., Small, E., Zreda, M., Calvet, J.-C., Crow, W., Kerr, Y. "Evaluation of the validated soil moisture product from the SMAP radiometer," (2016) *International Geoscience and Remote Sensing Symposium (IGARSS)*, art. #7729023, pp. 125-128. DOI: 10.1109/IGARSS.2016.7729023

Bi, H., Zeng, J., Zheng, W., Fan, X. "Validation of SMAP Soil Moisture analysis product using *in situ* measurements over the Little Washita Watershed," (2016) *Intl. Geoscience and Remote Sensing Symposium (IGARSS)*, art. #7729798, pp. 3086-3089. DOI: 10.1109/IGARSS.2016.7729798

Shellito, P.J., Small, E.E., Colliander, A., Bindlish, R., Cosh, M.H., Berg, A.A., Bosch, D.D., Caldwell, T.G., Goodrich, D.C., McNairn, H., Prueger, J.H., Starks, P.J., van der Velde, R., Walker, J.P. “SMAP soil moisture drying more rapid than observed *in situ* following rainfall events,” (2016) *Geophysical Research Letters*, 43 (15), pp. 8068-8075. DOI: 10.1002/2016GL069946

Zeng, J., Chen, K.-S., Bi, H., Chen, Q. “A Preliminary Evaluation of the SMAP Radiometer Soil Moisture Product over United States and Europe Using Ground-Based Measurements,” (2016) *IEEE Transactions on Geoscience and Remote Sensing*, 54 (8), art. no. 7457263, pp. 4929-4940. DOI: 10.1109/TGRS.2016.2553085

Chan, S.K., Bindlish, R., O'Neill, P.E., Njoku, E., Jackson, T., Colliander, A., Chen, F., Burgin, M., Dunbar, S., Piepmeier, J., Yueh, S., Entekhabi, D., Cosh, M.H., Caldwell, T., Walker, J., Wu, X., Berg, A., Rowlandson, T., Pacheco, A., McNairn, H., Thibeault, M., Martinez-Fernandez, J., Gonzalez-Zamora, A., Seyfried, M., Bosch, D., Starks, P., Goodrich, D., Prueger, J., Palecki, M., Small, E.E., Zreda, M., Calvet, J.-C., Crow, W.T., Kerr, Y. “Assessment of the SMAP Passive Soil Moisture Product,” (2016) *IEEE Transactions on Geoscience and Remote Sensing*, 54 (8), art. #7478653, pp. 4994-5007. DOI: 10.1109/TGRS.2016.2561938

Yee, M.S., Walker, J.P., Monerris, A., Rüdiger, C., Jackson, T.J. “On the identification of representative *in situ* soil moisture monitoring stations for the validation of SMAP soil moisture products in Australia,” (2016) *Journal of Hydrology*, 537, pp. 367-381. DOI: 10.1016/j.jhydrol.2016.03.060